~~CONFIDENTIAL~~

OFFICE OF SCIENTIFIC RESEARCH & DEVELOPMENT
NATIONAL DEFENSE RESEARCH COMMITTEE
DIVISION SIX - SECTION 6.1

CAVITATION NOISE
FROM
UNDERWATER PROJECTILES

AERONAUTICS LIBRARY
CALIFORNIA INSTITUTE OF TECHNOLOGY
PASADENA, CALIFORNIA 91125

THE HIGH SPEED WATER TUNNEL
CALIFORNIA INSTITUTE OF TECHNOLOGY
PASADENA, CALIFORNIA

SECTION Nº 6.1 - sr 207-1910
HML Nº ND-26

~~CONFIDENTIAL~~

COPY Nº 115

~~CONFIDENTIAL~~

OFFICE OF SCIENTIFIC RESEARCH AND DEVELOPMENT
NATIONAL DEFENSE RESEARCH COMMITTEE
DIVISION SIX – SECTION 6.1

CAVITATION NOISE

FROM

UNDERWATER PROJECTILES

ROBERT T. KNAPP

OFFICIAL INVESTIGATOR

THE HIGH SPEED WATER TUNNEL
AT THE
CALIFORNIA INSTITUTE OF TECHNOLOGY
HYDRAULIC MACHINERY LABORATORY
PASADENA, CALIFORNIA

Section No. 6.1-sr207-1910

HML No. ND-26

Report Prepared by
James W. Daily, Hydraulic Engineer
and
Howard Baller, Electronic Engineer

March 20, 1945

is document contains information affecting
e national defense of the United States within
e meaning of the Espionage Act, 50 U.S.C., 31
d 32, as amended. The transmission or the
velation of its contents in any manner to an
authorized person is prohibited by law.

~~CONFIDENTIAL~~

TABLE OF CONTENTS

CONFIDENTIAL

ABSTRACT

The High Speed Water Tunnel is operated by the California Institute of Technology under Contract OEMsr-207 with the Office of Scientific Research and Development, and is sponsored by Division 6, Section 6.1, of the National Defense Research Committee. The investigations reported here were authorized by a letter of October 23, 1042, from Dr. E. H. Colpitts, Chief of Section 6.1, National Defense Research Committee.

This report describes measurements of high frequency noise produced by projectiles cavitating in a high velocity stream of water. Spherical and ellipsoidal focusing reflectors were used in conjunction with a Brush C-11A hydrophone to locate the noise source. The main findings regarding the methods of measurement and the actual production of noise are:

1. Spherical and ellipsoidal reflectors produce good directivity characteristics and can be used to locate the region of the source of cavitation noise.

2. Measurements of the variation in sound emitted in the 20-100 kc band with the beginning and growth of cavitation on four different projectile shapes show:

    a. With the appearance of the slightest trace of cavitation the acoustic pressure increases to several times the magnitude of the background noise measured without cavitation.

    b. The maximum noise is measured when the zone of cavitation is limited to a very narrow band of very small bubbles.

    c. With further growth of cavitation the measured noise level drops gradually to approximately its initial value.

    d. The more abrupt the projectile profile, the more abrupt the increase in noise as cavitation begins.

    e. Cavitation which forms and collapses on the surface of the projectile causes the maximum noise at a K value very close to the inception point, while for cavitation which collapses in water away from the projectile surface, some additional reduction in K is necessary to cause maximum noise.

3. For the hemisphere nose the maximum noise intensity measured in any frequency band is approximately proportional to the velocity.

CONFIDENTIAL

4. Measurements to show the location of the noise source indicate:

   a. The main sound source is in the region of the trailing edge of the cavitation zone where the vapor bubbles are collapsing.

   b. The source moves downstream as the zone of bubbles develops.

   c. If the cavitation vapor bubbles are entrained and swept downstream before collapsing, the noise level drops.

CONFIDENTIAL

CAVITATION NOISE FROM UNDERWATER PROJECTILES

I. PURPOSE AND SCOPE OF THE INVESTIGATION

This report is the second in a series describing the results of a study of the sound produced at supersonic frequencies by projectiles cavitating in a high velocity stream of water.[1] The central purpose of this study was to determine the variation of sound emitted with the beginning and growth of cavitation on projectiles. The report describes a series of measurements using sound focusing reflectors in conjunction with the hydrophone and includes discussions of the following:

1. Characteristics of sound reflectors for cavitation noise measurements.
2. Measurements of the variation in sound emitted with the beginning and growth of different types of cavitation.
3. Location of the source of sound during cavitation.

The tests included measurements of noise in the 20--100 kilocycle frequency range produced by four different projectile shapes, each at zero yaw angle.

II. THE APPARATUS

The noise measurements were made in the High Speed Water Tunnel at the California Institute of Technology.[2] Two-inch diameter model projectiles supported in the 14 inch diameter working section were made to cavitate by increasing the velocity of the water or by decreasing the static pressure. In Figure 1,

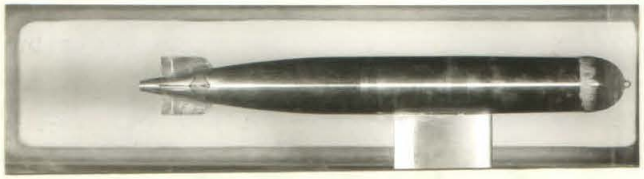

FIG. 1 TYPICAL INSTALLATION OF A PROJECTILE IN THE WORKING SECTION OF THE HIGH SPEED WATER TUNNEL SHOWING A BAND OF CAVITATION ON THE PROJECTILE NOSE

(1) Numbers in parentheses refer to references in Appendix II of this report

CONFIDENTIAL

which shows the installation of a projectile mounted on a special streamline strut, a typical ring of cavitation has been formed by the proper adjustment of pressure and velocity. Measurements of the noise emitted were made with a Brush C-11-A1 hydrophone placed opposite the projectile and outside the lucite window of the working section.

SOUND REFLECTORS

For the previous measurements described in Reference (1), the hydrophone was mounted in a water-filled blister clamped against one of the lucite windows of the tunnel working section. For measurements reported here, however, the hydrophone was used with focusing reflectors or "mirrors" and the hydrophone and mirror assembly was submerged in a water-filled tank which was attached to the side of the working section. The water was partially deaerated so as to avoid an accumulation of dissolved air bubbles on the hydrophone and window surfaces. Figures 2 and 3 show photographs of one installation used, and Figures 4 and 5 show a second installation. In both cases the hydrophone is located between a reflecting surface and the projectile. Noise originating on or near the surface of the projectile was transmitted through a water medium, continuous except for the lucite window, to the reflecting mirror and back to the hydrophone. Provisions were made in the supporting framework for moving the hydrophone-mirror assembly to any position inside the exterior tank, and for adjusting the focus of the hydrophone and mirror. This method offers several advantages over the previously used arrangement. The focusing effect helps isolate the source of noise and concentrates more of the total sound energy at the hydrophone. In reducing the reception from directions other than the focused direction, the possible interference from all sorts of standing wave effects is minimized. The hydrophone-mirror assembly was always focused with its axis normal to the working section window surface in order to avoid the attenuation obtained with oblique transmission through lucite.[3] The influence of this effect has been investigated only for flat sheets, whereas the interior surface of the window is cylindrical to conform to the working section 14" bore diameter. Consequently, for all but a horizontal plane the effect cannot be determined quantitatively. It might be noted that these transmission characteristics contribute indirectly to the focusing of any system, since, at a certain critical angle, the attenuation is complete and no sound is transmitted through the lucite sheet.

Two types of mirrors, as indicated in the above figures, were developed for these measurements. One had a spherical reflecting surface and the other, ellipsoidal. Both of these surfaces focus the sound coming from a single point on the axis of symmetry. The spherical mirror shown in Figures 2 and 3 was generated with a 12" radius and had a 10" aperture. The spacing of the elements of the system using this mirror determined by the relation:

$$\frac{1}{p} + \frac{1}{q} = \frac{2}{r}$$

where

p = distance from sound source to mirror surface

q = distance from hydrophone to mirror surface

r = radius of curvature of mirror surface

The ellipsoidal reflector shown in Figures 4 and 5 has a 1.9 to 1 ratio of major to minor axis and also has a 10" diameter aperture. Proper focusing is obtained if the sound originates at one focus of the ellipse and the hydrophone is placed at the other. For both nirrors the fraction received of the total noise emitted increases with the angle subtended by the reflector aperture.

CONSTRUCTION OF REFLECTORS

Different methods of construction were used for the two mirrors. The surface of the spherical unit is covered with a 1/8" layer of sponge rubber with nonintercommunicating air pockets. Figure 6 shows the face of this reflector with its rubber covering. The ellipsoidal reflector consists of two concentric copper shells separated by an air pocket. A view into the aperture, as in Figure 7, shows the "thick" construction due to this air pocket.

These constructions are based on the fact that the reflection of sound takes place when the waves strike a discontinuity in the transmitting medium. The percent of the incident sound pressure which is reflected is the ratio

$$\frac{\rho_1 C_1 - \rho_2 C_2}{\rho_1 C_1 + \rho_2 C_2}$$

where

ρ_1 and ρ_2 are the densities of Mediums 1 and 2

C_1 and C_2 are the velocities of sound in Mediums 1 and 2

The greater the difference between the products, ρC, the greater will be the reflection. Consequently, to obtain good reflection of sound traveling at a high velocity in a dense medium, the reflector should be a surface which forms a boundary with a low density substance in which sound travels slowly. Since the density of air is about one-eight hundreth the density of water, and the velocity of sound in air is about one-fifth that in water, both of the mirror constructions used satisfied the conditions for good reflection. The suggestion of an "air surface" for the reflector was made by W. D. Snow of the Columbia University Division of War Research.

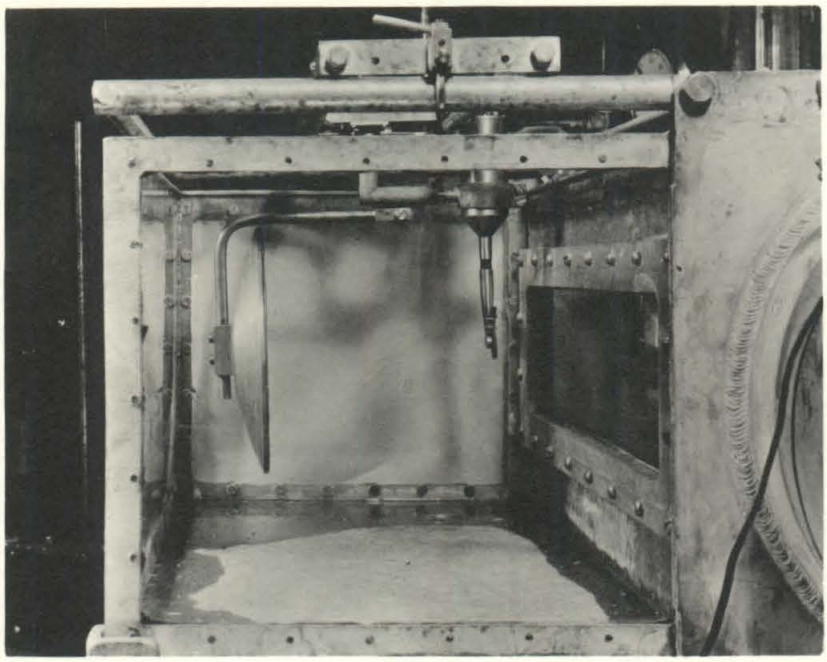

FIG. 2 SPHERICAL REFLECTOR AND C-11A HYDROPHONE ASSEMBLED IN WATER TANK AT WORKING SECTION SIDE WINDOW

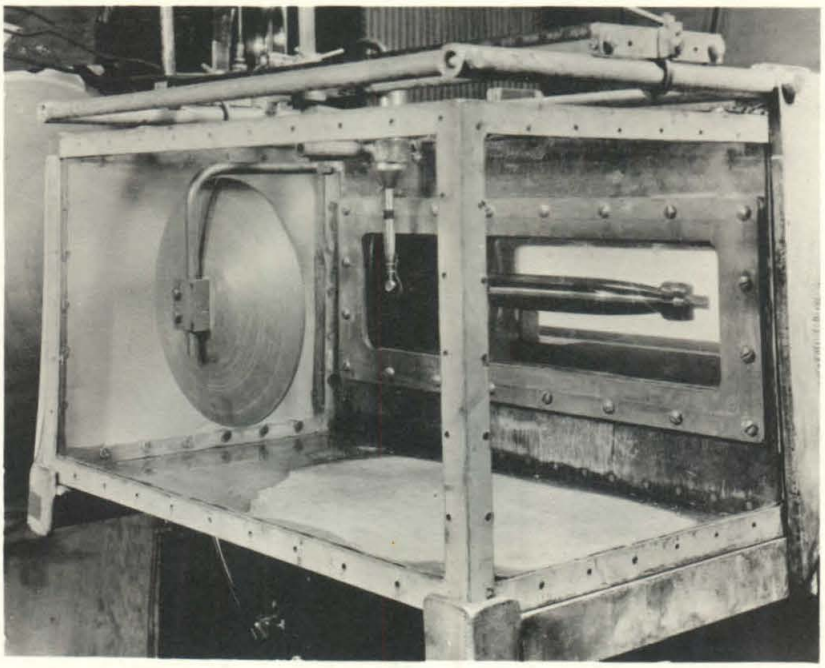

FIG. 3 SPHERICAL REFLECTOR AND HYDROPHONE ASSEMBLY FOCUSED ON PROJECTILE INSIDE WORKING SECTION
Note corprene shield on far face of hydrophone crystal head

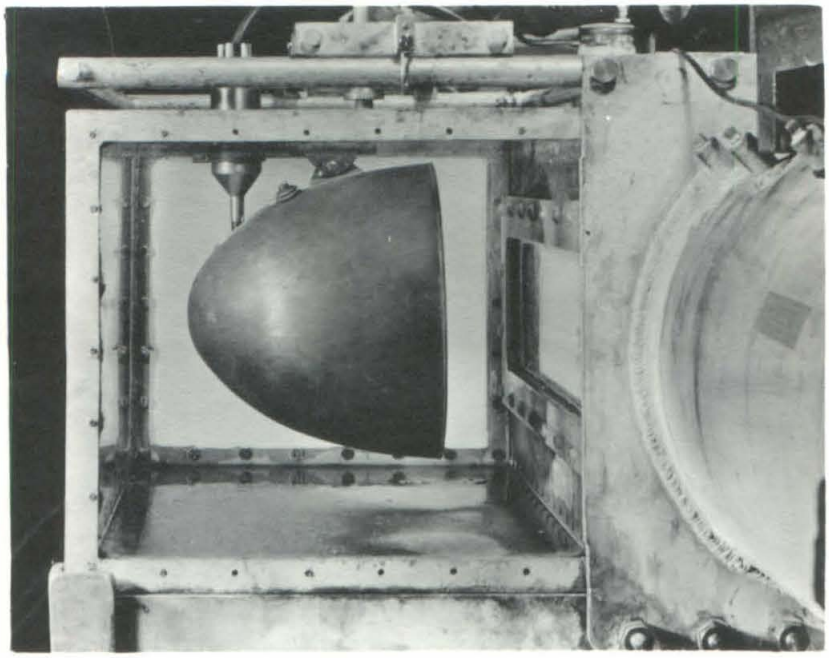

FIG. 4 ELLIPSOIDAL REFLECTOR AND C-11A HYDROPHONE ASSEMBLED IN WATER TANK AT WORKING SECTION SIDE WINDOW

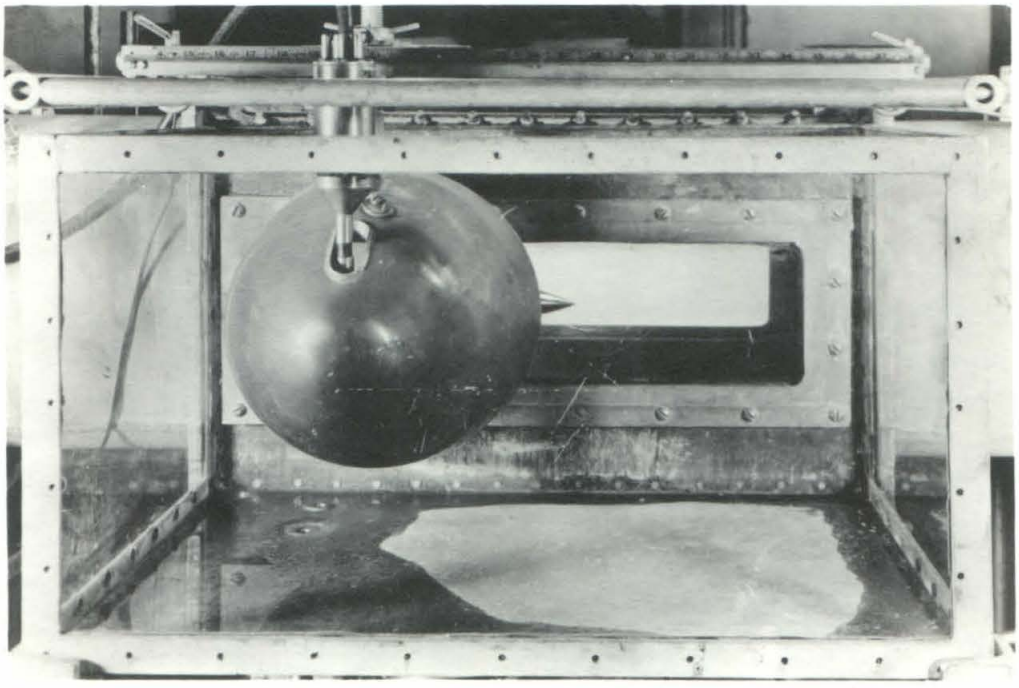

FIG. 5 ELLIPSOIDAL REFLECTOR AND HYDROPHONE ASSEMBLY FOCUSED ON PROJECTILE INSIDE WORKING SECTION
Note scale in upper part of photograph for positioning assembly with respect to projectile

HYDROPHONE SHIELDING

When using the spherical mirror the hydrophone was exposed and free to pick up sounds directly from other than the focused direction. Consequently, it was necessary to shield the exposed face and sides of the hydrophone crystal head and stem to avoid interference from these undesired directions. Thus, even in the focused direction, the hydrophone was shielded from direct radiation from the noise source and received only the noise reflected from the mirror surface. Corprene (cork impregnated duprene rubber) was used for this shielding, which is shown in Figures 2 and 3. With the ellipsoidal mirror, however, this hydrophone shielding proved unnecessary because the reflector itself limits the field of direct reception by the hydrophone to approximately 70 degrees. There was no possibility in this case for the hydrophone to receive energy from reflections off the tank walls surrounding the receiver assembly. Measurements with and without the shielding showed very little difference in directivity for the ellipsoid mirror with some reduction in gain with the corprene shield for a given source output.

For all measurements the hydrophone was oriented with the flat faces normal to the axis of focus. Following the convention of the "Dictionary of Underwater Acoustical Devices", (4) this is called zero degrees incidence.

SOUND MEASURING EQUIPMENT

As described in detail in Reference (1), the sound measuring equipment was designed to amplify the output of the detecting hydrophone in selected frequency ranges and to indicate the amplified voltage on a meter. As indicated in the diagram of Figure 8,

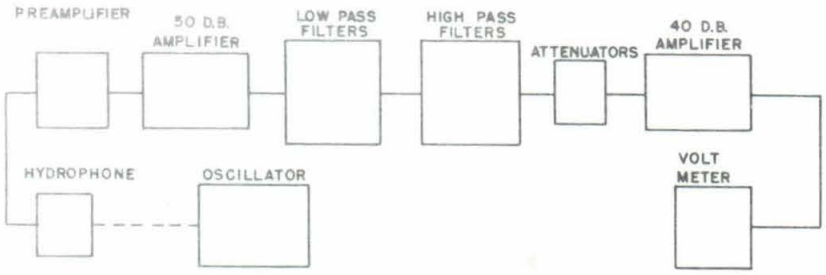

FIG. 8

the hydrophone output is fed into a cascade system of amplifiers, attenuators, and band pass filters which terminates in a vacuum tube voltmeter. Two filters were used in succession. One is a high-pass type with optional cutoff frequencies of 1, 5, 10, 20, 30, 40, 50, 60, 80, and 100 kilocycles. The other is a low-pass type with the same optional cutoff frequencies. With this arrangement channels of different widths and boundary frequencies can be chosen. The actual sound pressure in dynes per square centimeter is proportional to the voltage recorded.

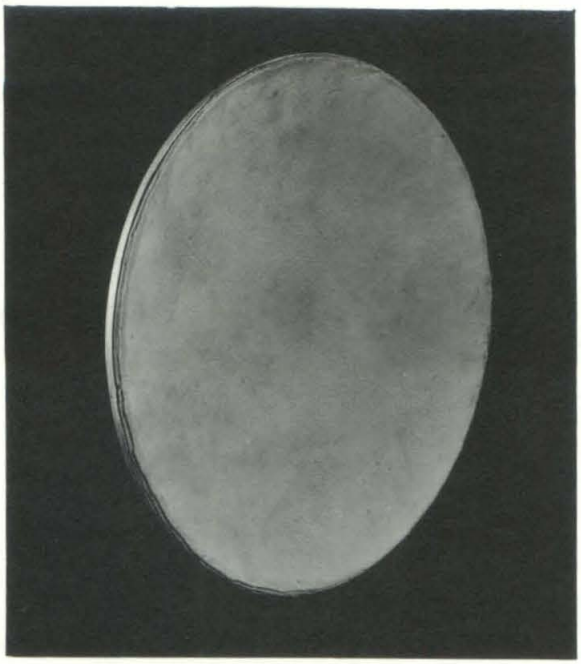

FIG. 6 FACE OF SPHERICAL REFLECTOR SHOWING SPONGE RUBBER COVERING

FIG. 7 VIEW INTO APERTURE OF ELLIPSOIDAL REFLECTOR AS ASSEMBLED FOR FIELD CALIBRATION.
A second C-11A Hydrophone (shown in foreground) is used as source and is rotated with respect to the mirror to obtain directivity pattern

III. SOUND REFLECTOR CHARACTERISTICS

FREE FIELD DIRECTIVITY PATTERNS

The directional characteristics of the hydrophone-mirror assemblies were checked by measuring the response in a free field for different given frequencies, and by comparing the focusing effects obtained with and without the reflectors when measuring noise from cavitating projectiles in the tunnel. A set of directivity patterns for the hydrophone alone and for the hydrophone with the spherical and elliptical reflectors was determined by the Calibration Group of the University of California, Division of War Research, at San Diego. The results, which included measurements over the 30 to 90 kc frequency range, are given in Reference (5), and typical patterns for the hydrophone with and without the ellipsoidal mirror are shown in Figures 9, 10, and 11. These calibrations duplicated the geometrical arrangement used for the Water Tunnel tests except that the lucite window between the source and the hydrophone-mirror assembly was not included, and no corprene shield was applied to the hydrophone crystal head to intercept direct radiation from the sound source. Because, as already mentioned, the latter omission is known to limit the effectiveness of the spherical mirror for Water Tunnel measurements, directivity patterns for this reflector are not shown. Reference again to Figure 7 shows the components of the elliptical mirror assembly arranged for calibration. Note that a second C-11 hydrophone (shown in foreground) was used as a sound source for the measurements. With its 9/16" diameter crystal head, it approximated a point source. Directivity patterns were obtained for two planes, one normal to both the reflector aperture and the receiving hydrophone stem, the other normal to the reflector aperture and containing the hydrophone stem. Figures 9 and 10 are for the first plane, Figure 11 is for the second.

As these figures show, the hydrophone alone shows some directional characteristics that increase with frequency. With the ellipsoidal reflector good directivity is obtained with the sharpness of the main lobe increasing with frequency. There is a tendency for secondary lobes to become more important at higher frequencies, a trend that is probably caused by the relatively large size of the receiving hydrophone crystal head with respect to the wave length at the higher frequencies. There is very little difference between the sets of curves for the two planes. The directivity index calculated by the method of Reference (4) from 50 kc and 70 kc curves in Figure 10 is -28 db and -31 db. This is 4 to 7 db better than the most directional hydrophone listed in the "Dictionary of Underwater Acoustical Devices."

CONFIDENTIAL

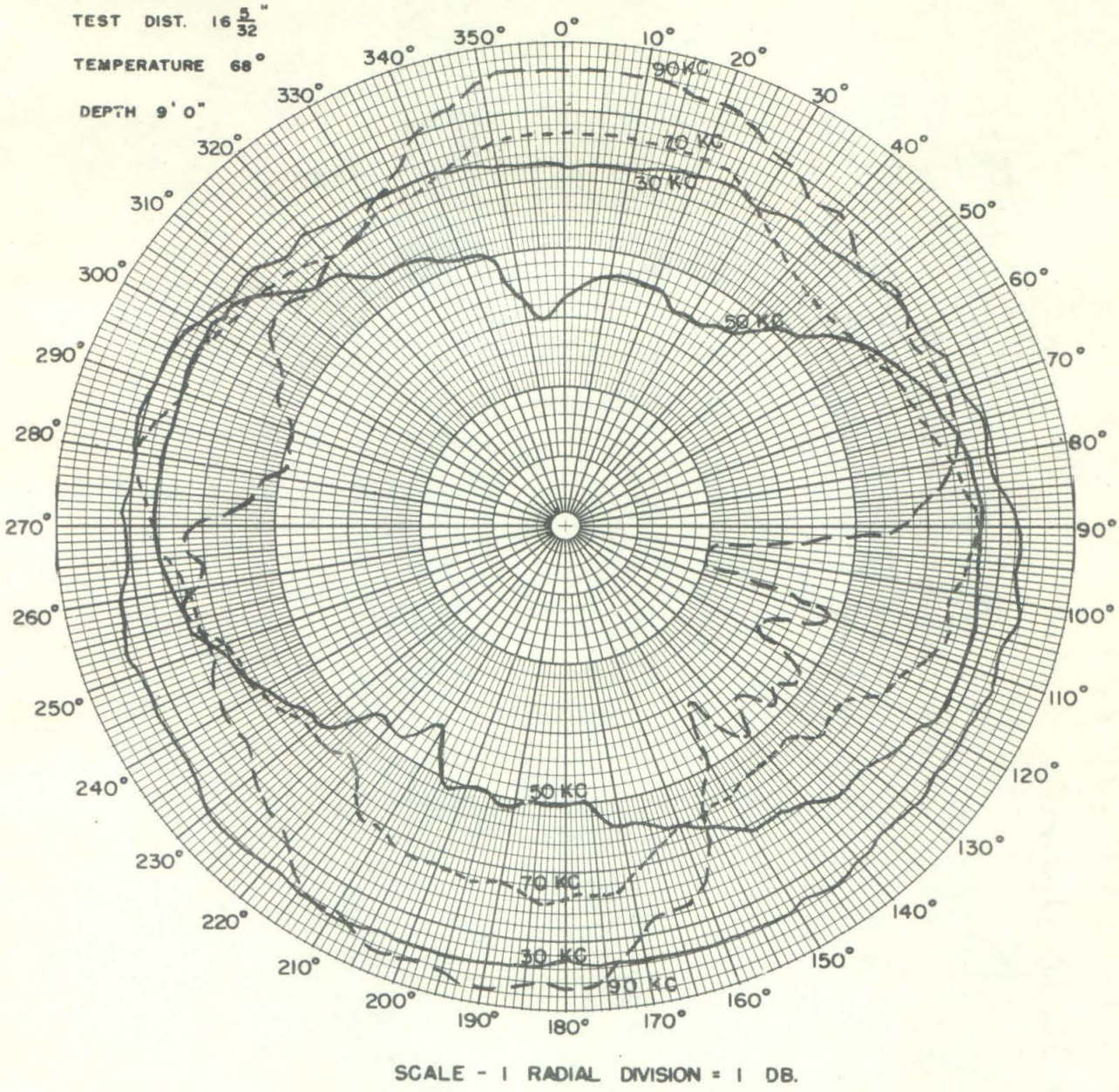

FIG. 9 C-11A HYDROPHONE

DIRECTIVITY PATTERNS IN PLANE NORMAL
TO HYDROPHONE SPINDLE

Data from Tests by University of California
Division of War Research. See Reference (5)

CONFIDENTIAL

CONFIDENTIAL

CONFIDENTIAL

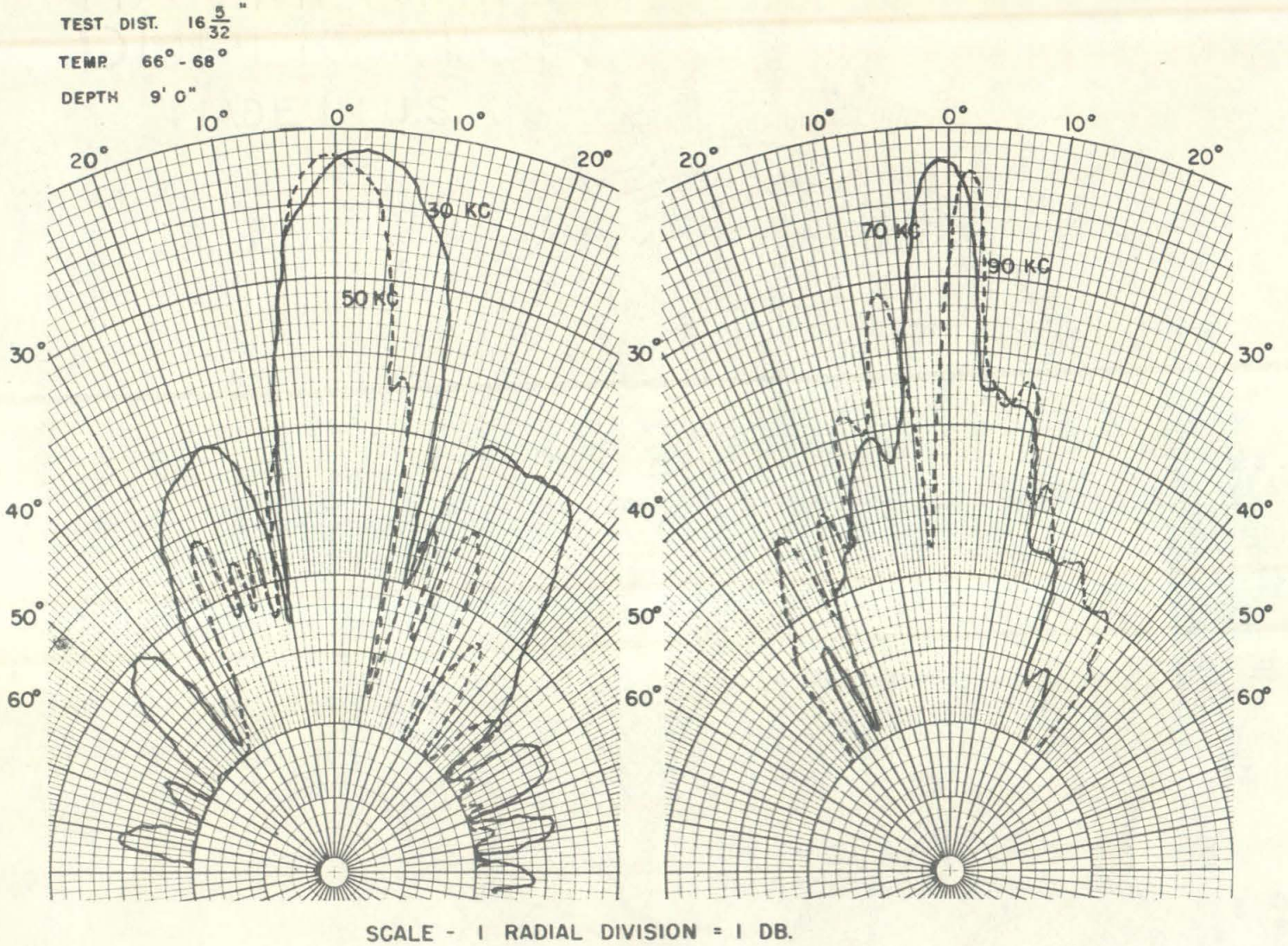

FIG. 10 C-11A1 HYDROPHONE WITH ELLIPSOIDAL REFLECTOR
DIRECTIVITY PATTERNS IN PLANE NORMAL
TO HYDROPHONE SPINDLE

Data from Tests by University of California
Division of War Research. See Reference (5)

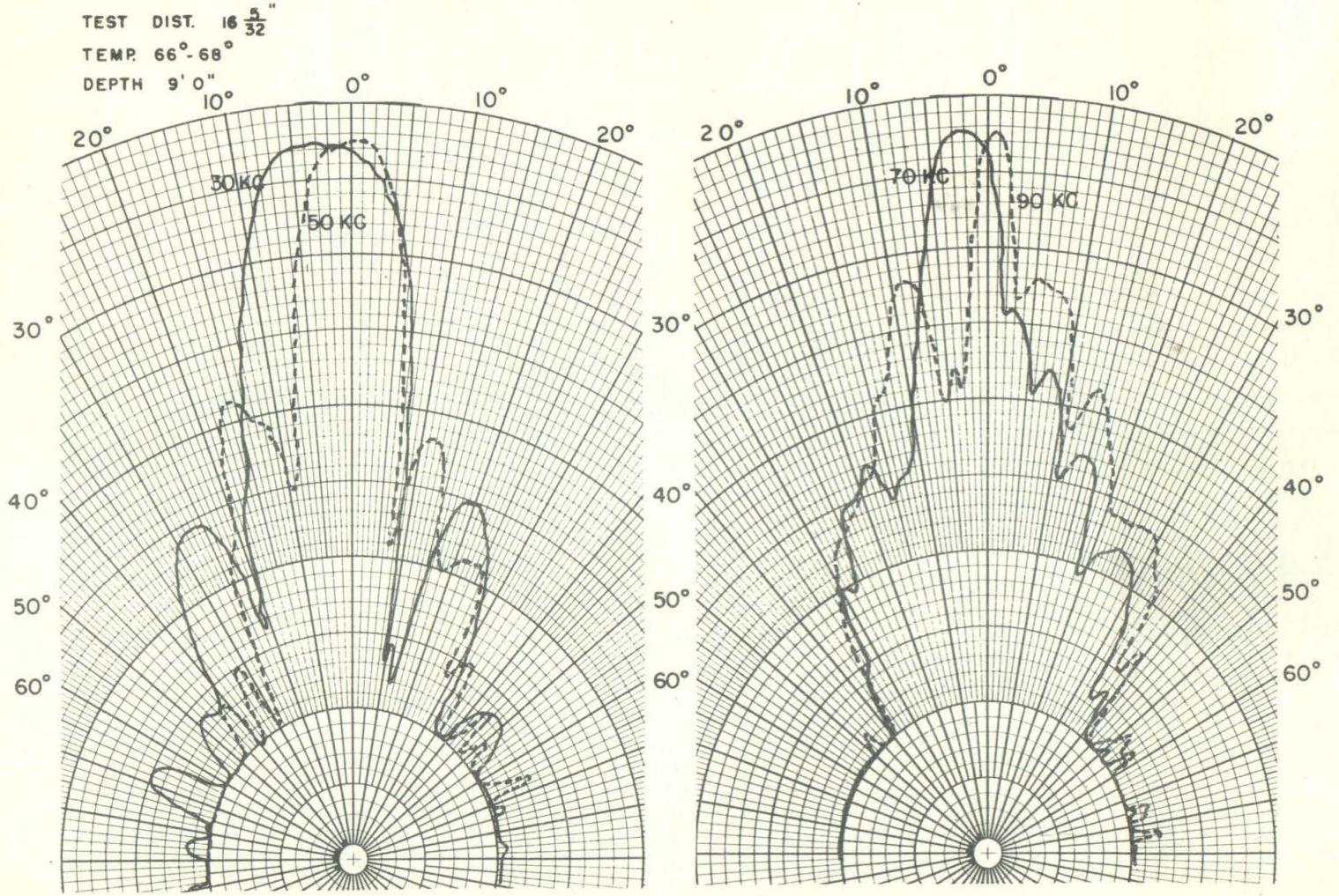

SCALE - 1 RADIAL DIVISION = 1 DB.

FIG. 11 C-11A1 HYDROPHONE WITH ELLIPSOIDAL REFLECTOR
DIRECTIVITY PATTERNS IN PLANE CONTAINING
HYDROPHONE SPINDLE
Data from Tests by University of California
Division of War Research. See Reference (5)

CONFIDENTIAL
CONFIDENTIAL

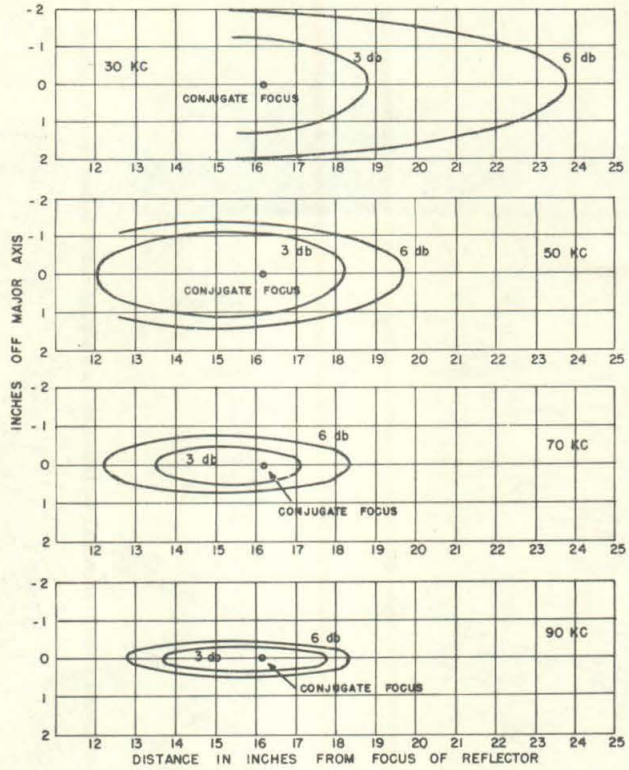

FIG. 12 LOCI OF SOURCE POSITIONS FOR HYDROPHONE RESPONSE 3 DB AND 6 DB BELOW INTENSITY MEASURED WITH SOURCE AT CONJUGATE FOCUS C-11A1 HYDROPHONE WITH ELLIPSOIDAL REFLECTOR
Data from tests by Univ. of Calif. Div. of War Research

LONGITUDINAL FOCUSING

The ellipsoidal reflector theoretically should indicate the maximum intensity for sound coming from its conjugate focus. Figure 12 shows the loci of source positions for 3 db and 6 db below the intensity measured with the source at the conjugate focus. These curves, also measured by the University of California Group, show the discrimination longitudinally to be from 1/5 to 1/3 as good as laterally. The effectiveness for both lateral and longitudinal directions increases with frequency. They also show the best focusing when the source is slightly short of the conjugate focus position.

Similar measurements with the spherical reflector have also indicated it to be much less sensitive in the longitudinal than in the lateral direction.

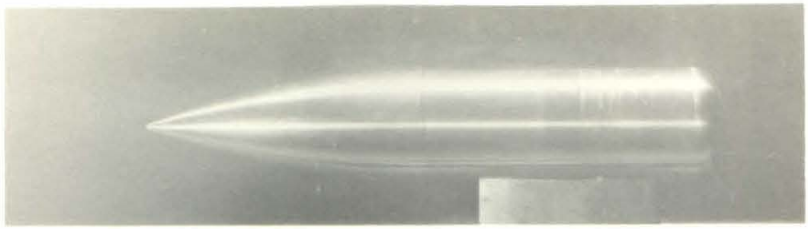

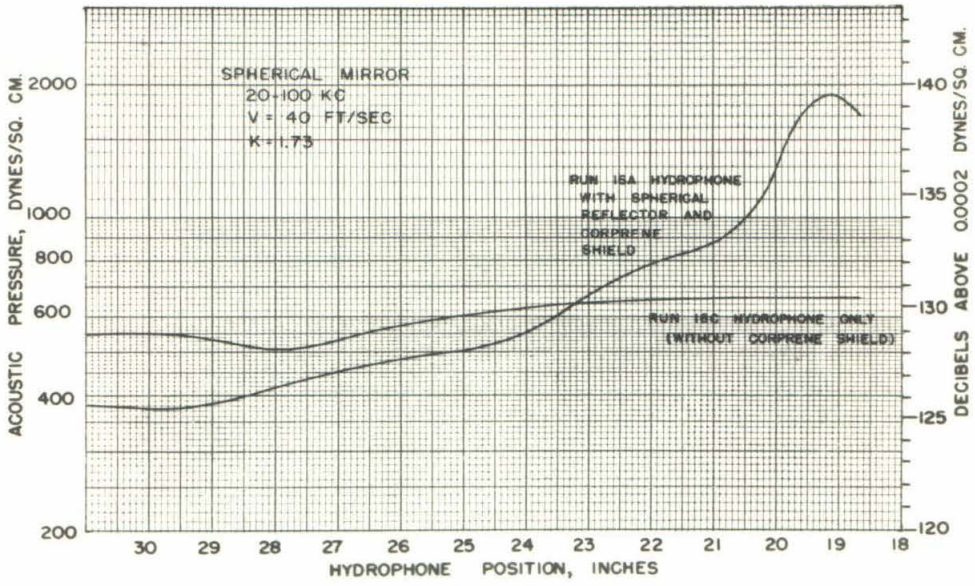

FIG. 13 EFFECT OF SPHERICAL MIRROR IN ISOLATING NOISE FROM CAVITATION ON THE SEMIELLIPSOID NOSE (Model 26.1-1)

GAIN AND FOCUSING FOR TUNNEL MEASUREMENTS

Using the arrangement shown in Figure 2 and with the hydrophone and mirror adjusted for the optimum focusing by the methods outlined on Page 2, measurements were made of the sound produced by a small ring of cavitation on a projectile nose. Following the test procedure described in Appendix I, the hydrophone-mirror assembly was moved parallel to the tunnel working section, and the location determined at which maximum noise was measured. Figure 13 shows a typical set of these measurements with the spherical mirror assembly compared with measurements obtained without the mirror. In this Figure the ordinate is sound pressure measured in the 20 to 100 kc band and designated by two scales; one a logarithmic scale of dynes per square centimeter, and the second a linear scale of decibels above the standard reference level of 0.0002 dynes per square centimeter. The abscissa is distance in inches measured parallel to the tunnel axis. The traverse is limited ahead of the nose by the length of the working section window through which the measurements were taken. The extent of the cavitation causing the noise is shown in the photograph above the curves. It will be noted that the ring on the nose is the only zone of cavitation, so that the source is concentrated. The pronounced focusing effect of the mirror is evident.

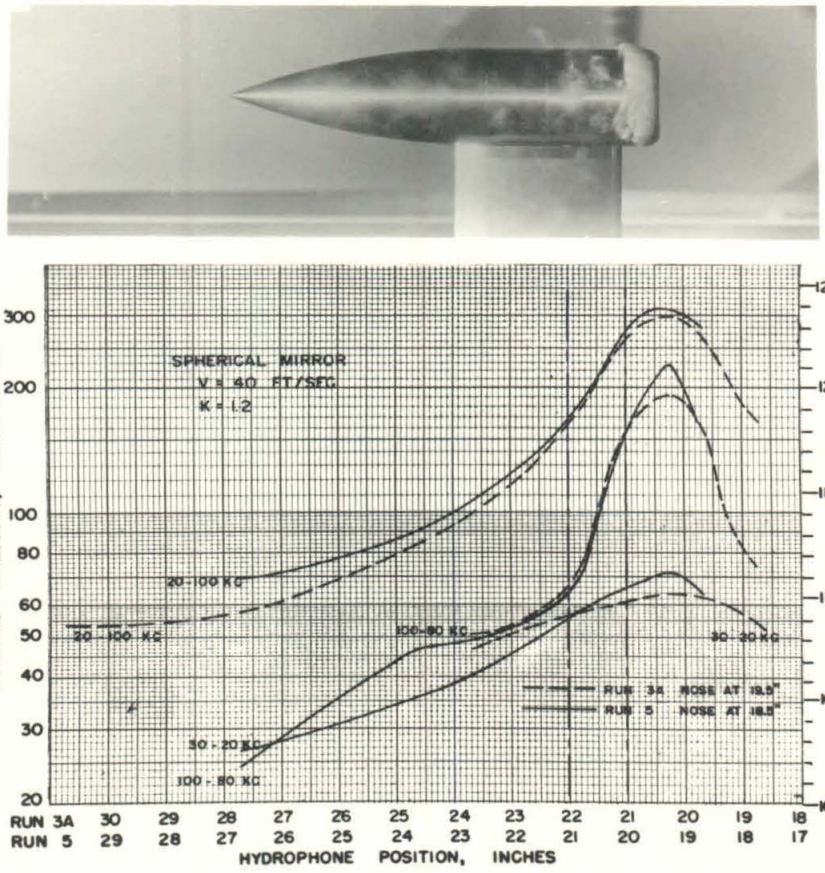

FIG. 14 INFLUENCE OF SHIFTING PROJECTILE POSITION ON EFFECT OF SPHERICAL MIRROR IN ISOLATING NOISE FROM CAVITATION ON THE TRUNCATED HEMISPHERE NOSE

Without the mirror there is a slight reduction in level as the hydrophone is moved away from the noise source. Adding the mirror gives a 9 db gain at the peak. As the mirror assembly is moved away from the source, the level falls sharply until finally the directivity feature results in so little pickup from the source that the level drops below that measured with the hydrophone only.

In Figure 14 are shown two sets of measurements on another projectile. The measurements were intended to be for identical conditions except for the position of the model on its supporting strut. Again, the amount of cavitation causing the noise for the projectile positioned as in Run 3a is shown in the photograph above the diagram. For Run 5 the projectile nose was one inch farther forward than for Run 3a. The data which are plotted to abscissa scales shifted by this amount show the noise peaks to fall at the same point relative to the model nose for both tests. Thus the focusing effect obtained is real and not dependent on the tunnel geometry. The influence of the supporting strut (as long as it does not cavitate) is also shown to be negligible. In addition, the curves show the noise peaks in frequency bands of

CONFIDENTIAL

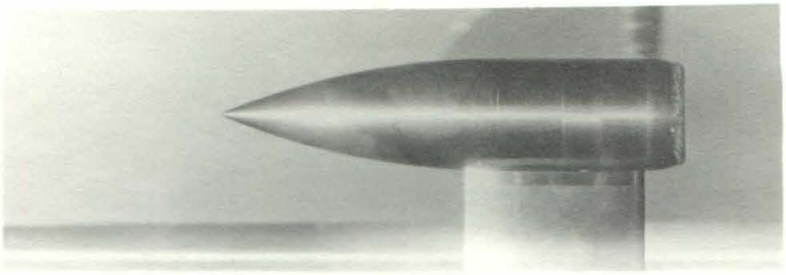

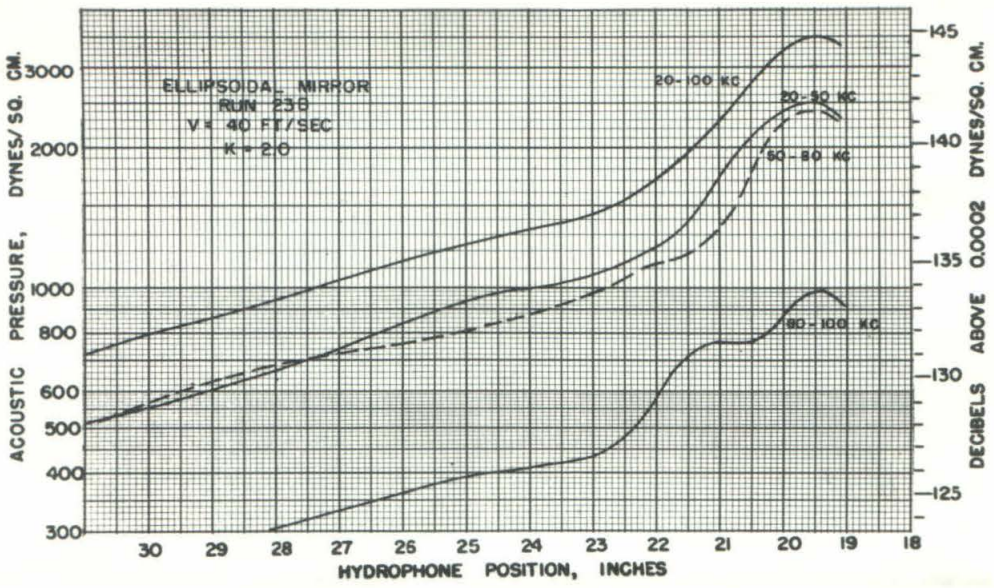

FIG. 15 EFFECT OF ELLIPSOIDAL MIRROR IN ISOLATING NOISE FROM CAVITATION ON THE TRUNCATED HEMISPHERE NOSE

20-100 kc, 80-100 kc, and 20-30 kc to fall at the same point relative to the model nose. The most pronounced focusing is obtained with the highest frequency band. Focusing in the low frequency band is definite but not as sharp. Consequently, the curves for the entire 20-100 kc range, which is made up of approximately the root-mean-square values of the noise in all the frequencies, shows a peak with a sharpness intermediate between those for the high and low bands. This effect of high frequency on sharpness of focus is probably explained by the increased ratio of mirror aperture to wave length.

Measurements on the same model but using the ellipsoidal reflector are shown in Figure 15. With this mirror there is a gain in measured sound level several times that obtained with the spherical mirror. While an exact comparison is not possible because the two curves are for different degrees of cavitation, an order of magnitude of nearly ten to one is indicated. Otherwise the focusing effects of the mirror are similar to those of the spherical reflector. The same trend in the effect of frequency on sharpness of focus is also obtained.

IV. BACKGROUND NOISE

The measurements of sound from cavitating projectiles in the tunnel working section include, of course, a certain amount of "background" noise generated by the tunnel flow circuit and its mechanical drive. To be sure that over the frequency range of interest the magnitude of this noise was small relative to the cavitation noise, a series of measurements was made without the model or its supporting strut in the working section. With the hydrophone-mirror assembly focused on a fixed point on the tunnel axis, noise was measured over a wide pressure range for different constant velocities.

EFFECT OF VELOCITY AND PRESSURE

The typical curves shown in Figure 16 illustrate the magnitude of the background noise and the effect of velocity and pressure on the noise. In this figure measurements for velocities of 40 to 70 feet per second are plotted as a family of curves of sound pressure in dynes per square centimeter (with linear decibel scale) vs. the cavitation parameter, "K". The data were obtained from two sets of tests, both with spherical mirror and with the sound filters set to include the entire 20 to 100 kc band. These curves show the same characteristic trends as were obtained by the

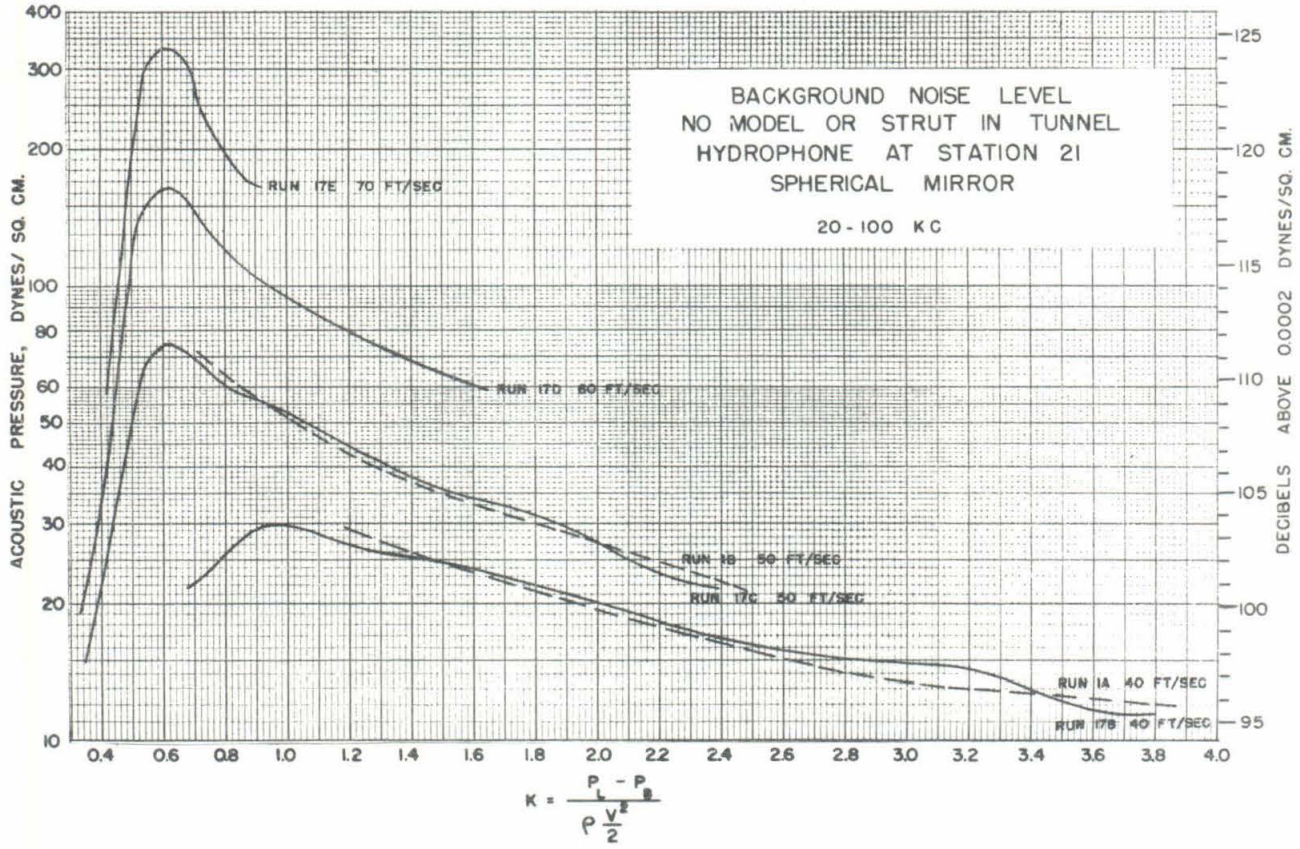

FIG. 16

earlier measurements without a reflector described in Reference (1). For each velocity, as the pressure is reduced from an initially high value, the increased tendency for flow separation and cavitation in various parts of the flow circuit caused an increase in noise until at a low K a peak is reached and the level drops off. The sudden reduction in this figure coincides with cavitation in the contracting nozzle at the entrance to the working section, and an accumulation of vapor and air bubbles which clouded the working section.

EFFECT OF TUNNEL CIRCUIT VARIABLES

The data plotted in Figure 16 could be duplicated as long as tunnel conditions remained the same. However, changes in the condition of the circulating pump, changes in relative settings of the valves in the pressure control circuits auxiliary to the tunnel, and, of course, any change in the flow circuit itself, caused some variation in the magnitude of the background noise. Differences of as much as 10 db have been observed for the same combination of these variables. Figure 17 shows the results obtained with the spherical mirror assembly but at a later date than

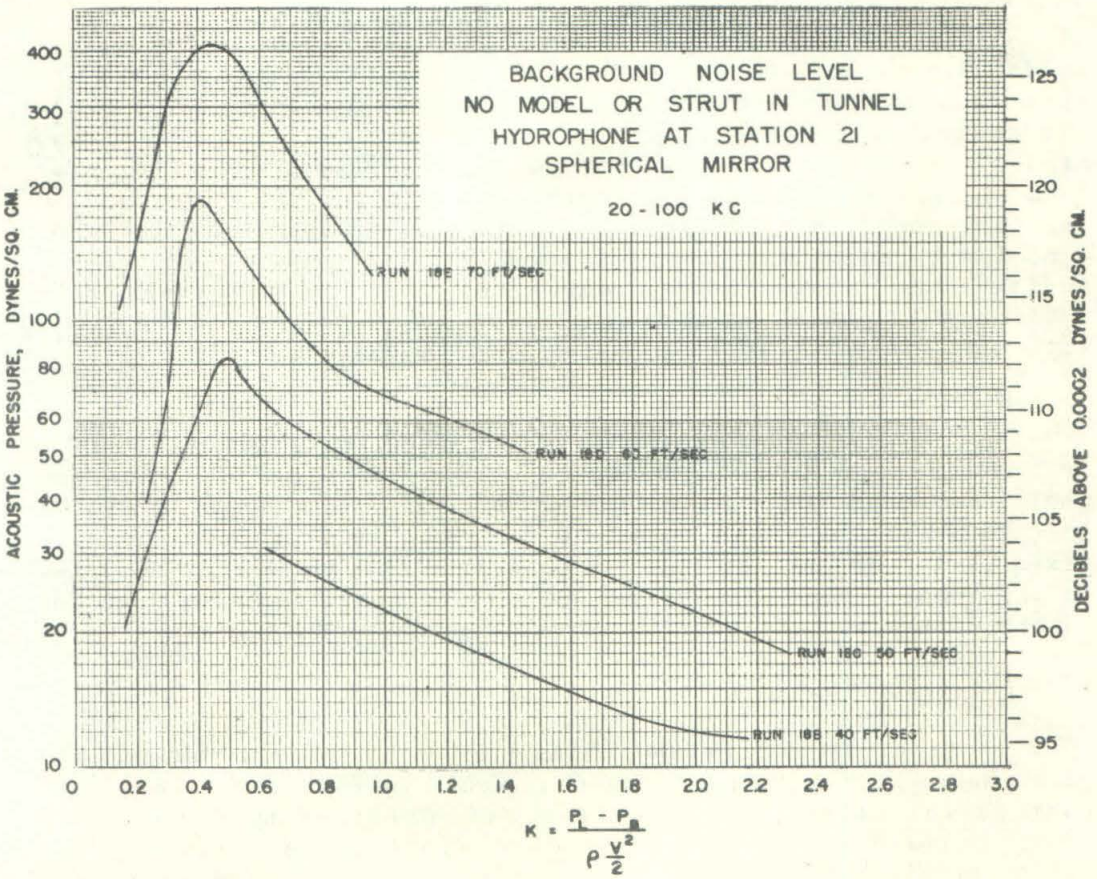

FIG. 17

for Figure 16 and with an improved contracting nozzle at the inlet to the working section. These curves are similar to those in Figure 16 but show from 2 to 5 decibels lower noise levels at the same K. Also, a lower K is reached before the noise drops. In this case no nozzle cavitation was obtained, but with sustained operation at the low absolute pressures corresponding to the lowest K values, an accumulation of air was obtained in the tunnel and the noise level dropped.

BACKGROUND NOISE VS. CAVITATION NOISE

The highest sound pressure measured in the clear tunnel at 70 ft/sec, the maximum velocity at which noise from projectiles was recorded, was about 420 dynes per square centimeter. As will be discussed later, pressures of 1000 to 2000 dynes per square centimeter were measured with the spherical mirror as cavitation developed on the projectile shapes. Since the recorded level is approximately the root-mean-square value of all the sound contributions, the background noise has no significant effect on these pressures. It is possible also, for the same reason, to ignore the relatively small effect of background noise variations caused by different tunnel setups as illustrated by the two figures, 16 and 17.

Similar background noise measurements made using the ellipsoidal mirror showed 5 to 8 decibels higher levels than with the spherical mirror. However, peak noise pressures of 5000 dynes per square centimeter or greater were measured from cavitating projectiles with this reflector making the background noise even less significant. It is interesting to note that for the particular test conditions of Figures 16 and 17, and for K greater than 0.6, the background sound pressure is approximately proportional to the fourth power of the water velocity and inversely proportional to the water pressure. For low K values nozzle cavitation or air accumulation changes this relationship.

UNIFORMITY OF BACKGROUND NOISE

A comparison of the background noise obtained at different positions along the center line of the tunnel is shown in Figure 18. These measurements were made with the velocity and pressure fixed (K = constant) by moving the hydrophone and mirror parallel to the tunnel axis. They show the same noise level throughout the length of the working section normally occupied by the model.

BACKGROUND NOISE WITH PROJECTILE IN TUNNEL

In order to verify that these "clear tunnel" measurements gave the same background noise that would be obtained with actual test installations, a projectile was installed in the working section and a survey made for noncavitating conditions. With V = 40 ft/sec and K = 3.74, the conditions of test used to obtain the data in Figure 16 were duplicated as nearly as possible and measurements made of noise vs. distance along the tunnel axis.

With such a high value of K no cavitation existed at any place on the model. These measurements shown in Figure 19 gave an average noise level within 2 db of the clear tunnel noise shown for the same K in Figure 16.

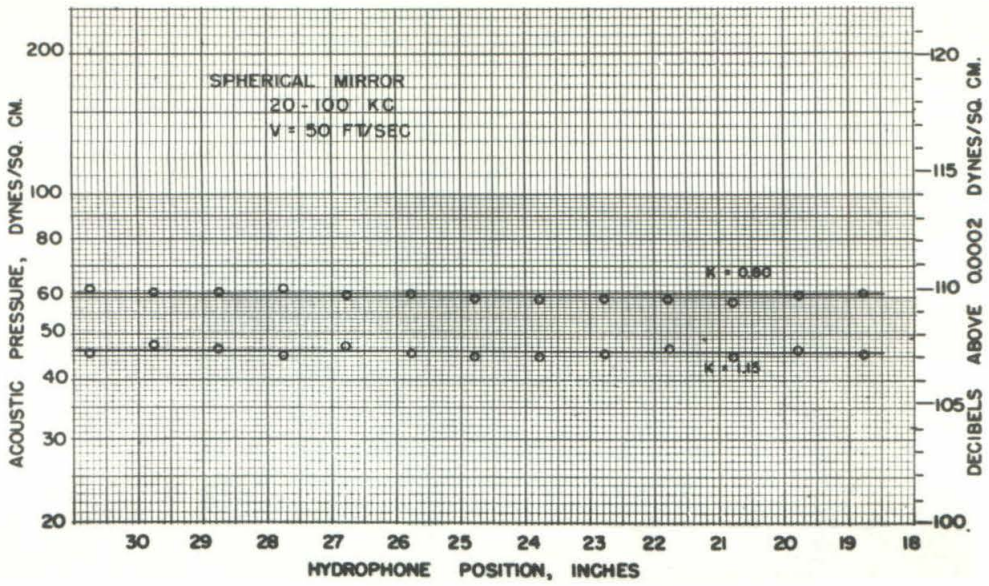

FIG. 18 BACKGROUND NOISE LEVEL AT DIFFERENT POSITIONS ALONG CENTERLINE OF TUNNEL
No model or strut in tunnel

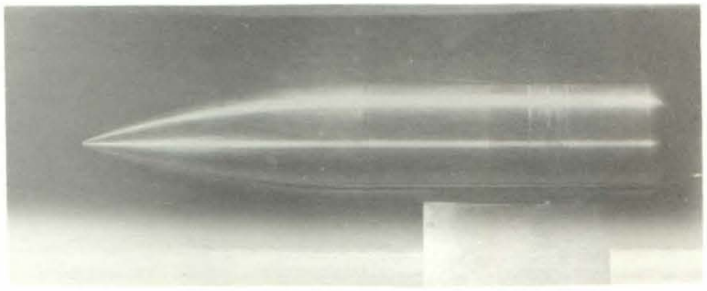

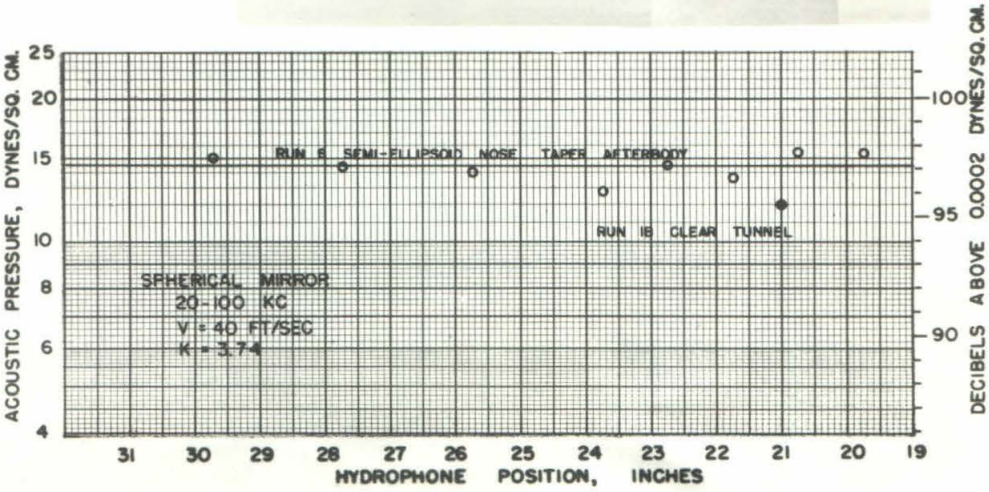

FIG. 19 BACKGROUND NOISE WITH MODEL IN TUNNEL
SEMIELLIPSOID NOSE
(Model 26.1-1)

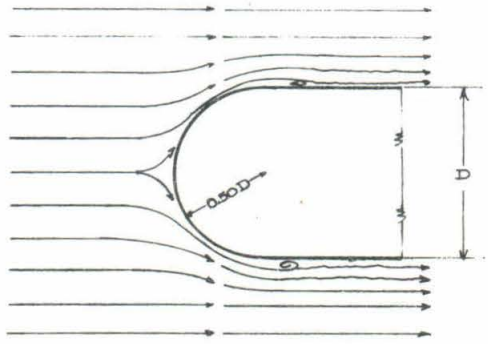

HEMISPHERE NOSE

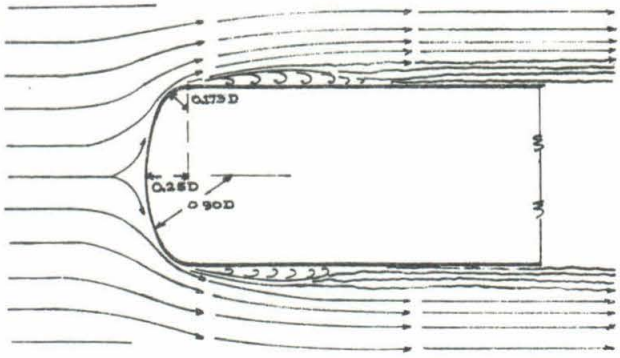

SEMIELLIPSOID NOSE

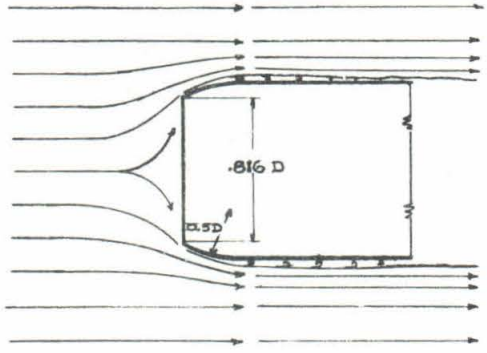

TRUNCATED HEMISPHERE NOSE

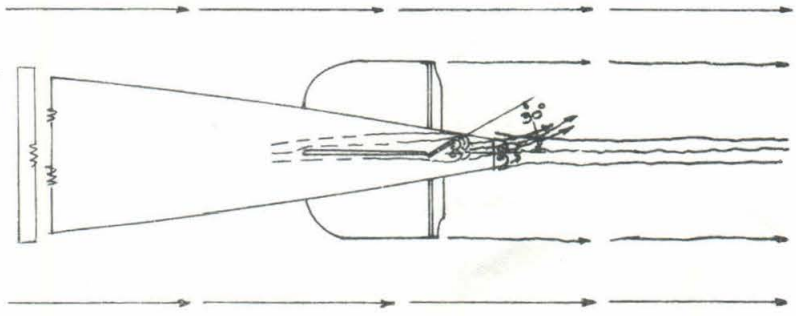

UPTURNED TAIL RUDDER ON
PROJECTILE AFTERBODY

FIG. 20 PROJECTILE PROFILES WITH FLOW DIAGRAMS

V. MEASUREMENTS OF NOISE PRODUCED BY CAVITATING PROJECTILES

A. CORRELATION WITH THE BEGINNING AND GROWTH OF CAVITATION

CAVITATION TYPES AND INFLUENCE OF PROFILE SHAPE

During observations of various projectiles in the Water Tunnel, it was noticed that as cavitation first appeared, the formation and collapse of the cavitation bubbles were different for varying degrees of abruptness of the body at the cavitation zone. Where the profile was not too abrupt, the zone of cavitation bubbles appeared to form, grow, and collapse right on the surface of the body. For more abrupt bodies the bubbles seemed to form at the surface of the body, but to spring clear of the body before collapsing and disappearing. For some very abrupt shapes the cavitation vapor pocket originated and collapsed in the stream away from the disturbing surface and with no visible connection to the body itself. Consequently, in studying the correlation of sound generated with the beginning and growth of cavitation, the several different forms of cavitation were investigated by using several body shapes. The four bodies for which measurements are reported here and the type of *incipient cavitation* obtained are listed below:

1.	Hemisphere Nose	Cavitation forms and collapses on the surface of the projectile
2.	Semiellipsoid Nose	Similar to above
3.	Truncated Hemisphere Nose	Cavitation vapor bubbles originate at the sharp edge but collapse in the stream away from the projectile surface
4.	Tail Rudder Tilted into Stream	No visible connection between cavitation bubbles, which form and collapse in water, and the rudder surface

A comparison of the shapes of the four bodies and the types of flow about each for noncavitating conditions are shown by the scale drawings in Figure 20. The three noses and the upturned rudder present to the flow successive changes from smooth to blunt and abrupt profiles. The flow line diagrams, which were drawn from detailed observations of the actual flow in the Polarized Light Flume, [2] are useful for qualitatively determining the pressure field around the projectile and, hence, locating the zones of low pressure where cavitation is most likely to occur Wherever the

flow, which has been pushed aside by the projectile surface, begins to curve back around the body (concave towards the body), local reductions in pressure are affected. The greater this curvature, the lower the pressure and the greater the possibility of developing cavitation. The flow lines show the maximum curvature near the junction between nose and cylinder for the hemisphere and semiellipsoid noses at the sharp edge on the truncated hemisphere, and at the tip of the rudder on the finned afterbody. In addition, the diagrams show varying sharpness in maximum curvature, indicating earliest cavitation for the truncated hemisphere nose or upturned rudder, and later cavitation for the semiellipsoid and hemisphere noses.

SOUND PRESSURE VS. CAVITATION GROWTH

With the hydrophone and spherical mirror focused on the zone of incipient cavitation and using the test procedure outlined in Appendix I, curves showing the variation in sound pressure with the amount of cavitation were obtained for each projectile. A corresponding series of photographs showing the successive stages of cavitation development were also made. All tests were made with zero yaw and zero pitch. The results are shown in Figures 21, 22, 23, and 24 where the sound pressure is plotted against the cavitation parameter. A scale for the sound level in decibels is also shown. The photographs included in the same figures are arranged in the order of decreasing values of K and each is marked with the corresponding measured sound level. Note that in all cases the total sound in the 20 to 100 kc band is shown, but that the data for each nose were obtained at a different constant velocity.

Each set of curves and photographs in Figures 21 to 24 show the following common characteristics:

1. With reduction in the cavitation parameter, K, the sound pressure rises sharply to several times the magnitude of the background noise in the tunnel as soon as the slightest trace of visible cavitation is observed.

2. The rise in sound begins with the appearance of minute cavitation bubbles and reaches a peak value while the ring of bubbles is still very narrow.

3. The sound pressure decreases with continued development of cavitation until, for fully developed conditions, the noise is but a fraction of the peak magnitude. For some cases it drops to approximately the same level as the tunnel background noise.

These characteristics are shown clearly by examining Figure 21 for the hemisphere nose. For high values of K at which no cavitation occurs on the projectile, the measured noise is only that due to background disturbances. However, as K is reduced by reducing the hydraulic pressure or increasing the velocity, and

cavitation begins, the noise rises sharply to a high value. In this instance the increase is from 95 to 1700 dynes per square centimeter, a gain of about 25 db. With continued growth of cavitation the noise peaks and then falls off until, with very large bubbles enveloping the body, the measured level equals the background noise level. During tests at the K corresponding to Figure 21 (a), only small intermittant bubbles of cavitation could be discerned by careful visual examination. They were too small to be detected photographically. Figure 21 (b) shows a small amount of cavitation along the top half of the body at the junction between the hemisphere and the cylinder. Note that it is a very narrow band, yet as the noise curve shows, it is between this condition and the slightly more developed one shown in the next photograph that the maximum noise is measured.

Examination of Figure 22 shows the semiellipsoid nose to cavitate at a higher K, but otherwise to exhibit the same characteristics. Because the background noise was very low for this 40 ft/sec test, the noise gain at the inception of cavitation is nearly 37 db. Again, as indicated in Figures 22 (b) and 22 (c), the maximum noise is measured with only a thin ring of cavitation near the junction between the cylindrical body and the nose contour. A second small noise peak of undetermined cause is evident at K = 1.0 when a relatively wide zone of cavitation exists.

Figures 21 and 22 both showed similar types of incipient cavitation where the bubbles lay close to the body surface. Figure 23, for the truncated hemisphere nose, shows the second type of cavitation where the bubbles collapse in the water away from the body. Figures 23 (a) and 23 (b) illustrate this clearly. The trailing ends of the small cavitation wisps which originate at the sharp edge on the nose are separated from the body by a definate space. With continued growth of cavitation, the bubble zone becomes more dense and this characteristic is less discernible. The same trends in measured sound were obtained as for the other two noses with about a 23 db increase in level as cavitation began.

Figure 24 shows sound measurements and photographs for a tail rudder tilted up into the stream. As the first photographs of the series show, the initial cavitation occurs at the rudder post as well as at the tip and finally, at very low K values, the entire wake behind the tilted rudder becomes filled with vapor. The noise curve shows the characteristic increase to a peak value and then reduction with cavitation growth. Note that, as Figure 24 (d) shows, the peak noise, a 40 db gain over the background, is obtained with very little visible cavitation.

These measurements confirm the results obtained without the focusing device and which have already been reported.[1] With the focusing system, however, the sensitivity of the noise measurements was increased so much that the detection of the onset of cavitation was more definitely marked, leading to a much sharper rise in the measured sound pressure curve.

It might be noted that surface condition is very critical in making the cavitation measurements. The noise measurements and cavitation photographs of the four noses were made after carefully polishing the assembled models and wiping the surface and joints between body sections with a waxed cloth. These precautions caused the onset of cavitation to be more uniform by eliminating early cavitation at isolated points around the periphery of the projectile.

SOUND PRESSURE AND BUBBLE COLLAPSE

The fact that for all three types of cavitation the maximum sound was measured when the visible cavitation was small and that the magnitude was reduced with the growth of the bubbles, might be tied in with the concept that the noise originates primarily at the bubble collapse. With small cavitation bubbles which form and collapse cleanly and sharply within a small physical zone, the energy release and, hence, the noise is of high intensity. As the zone of cavitation grows, the bubbles collapse throughout a larger space and mutual interference and absorption due to the damping properties of the bubbles themselves reduces the intensity of the noise radiated.

CONFIDENTIAL

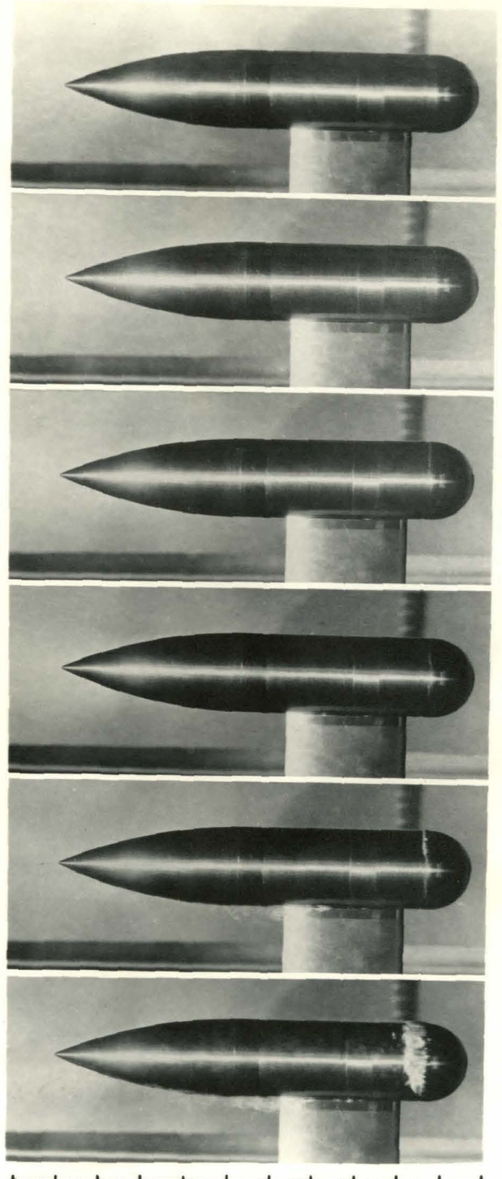

(a)

K = 0.79

SOUND = UNSTEADY NOISE LEVEL DUE TO INTERMITTANT CAVITATION.

(b)

K = 0.77

SOUND = 137 db

(c)

K = 0.73

SOUND = 139 db

(d)

K = 0.68

SOUND = 138 db

(e)

K = 0.65

SOUND = 135 db

(f)

K = 0.60

SOUND = 130 db

29 28 27 26 25 24 23 22 21 20 19 18

DISTANCE ALONG AXIS, INCHES

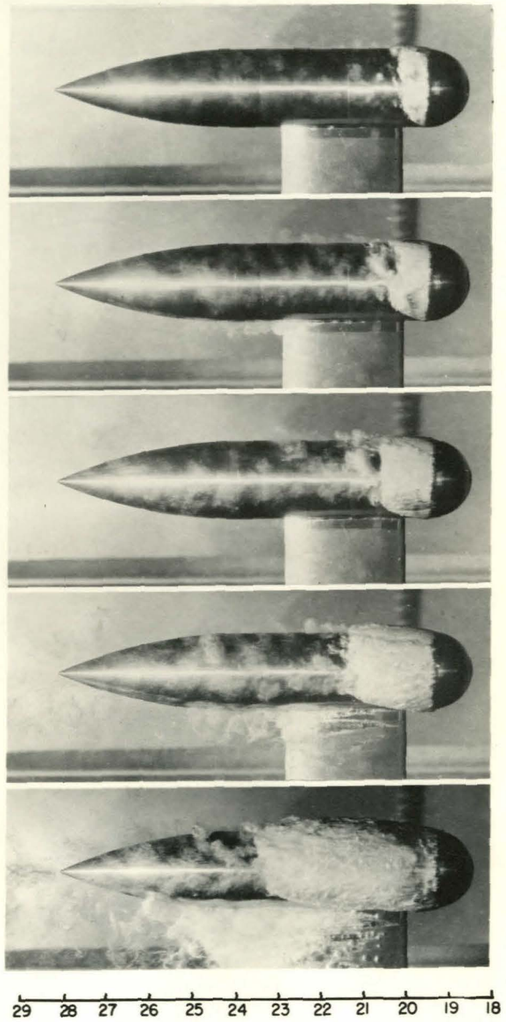

(g)

K = 0.56

SOUND = 129 db

(h)

K = 0.50

SOUND = 128 db

(i)

K = 0.45

SOUND = 125 db

(j)

K = 0.41

SOUND = 123 db

(k)

K = 0.31

SOUND = 115 db

29 28 27 26 25 24 23 22 21 20 19 18

Fig. 21

CAVITATION ON HEMISPHERE NOSE

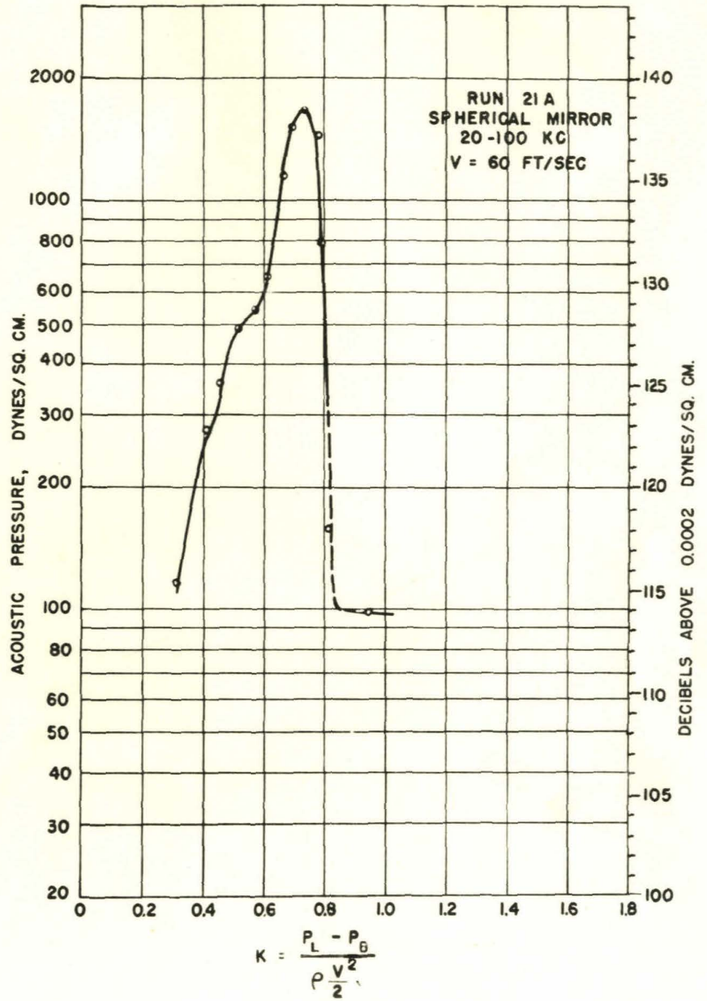

CONFIDENTIAL

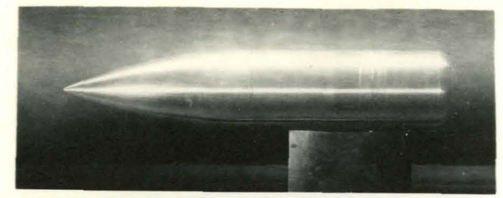

(a)

K = 2.55

SOUND = 96 db

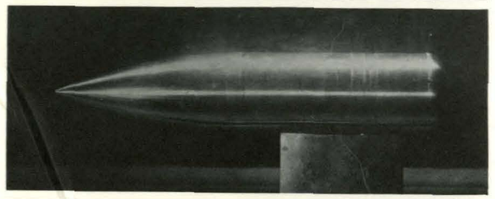

(b)

K = 1.82

SOUND = 138 db

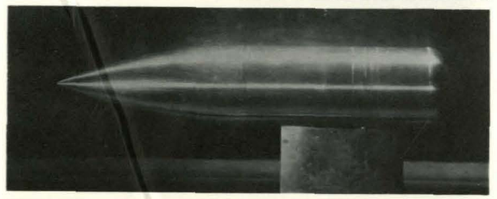

(c)

K = 1.74

SOUND = 138 db

(d)

K = 1.52

SOUND = 131 db

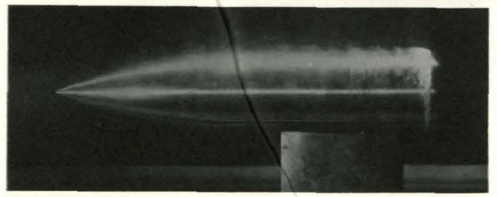

(e)

K = 1.29

SOUND = 129 db

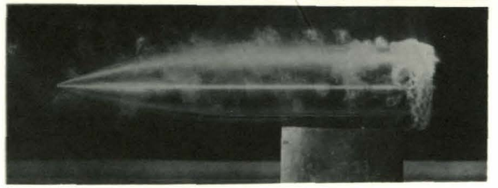

(f)

K = 1.03

SOUND = 127 db

29 28 27 26 25 24 23 22 21 20 19 18

DISTANCE ALONG AXIS, INCHES

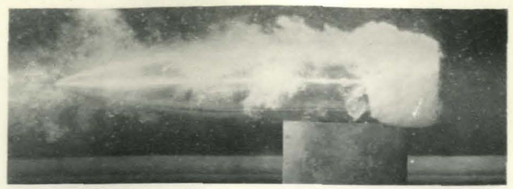

(g)

K = 0.71

SOUND = 120 db

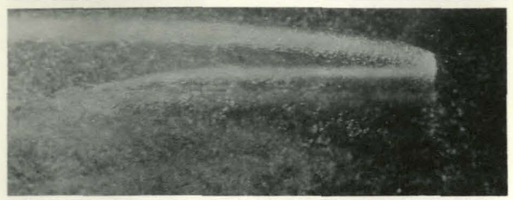

(h)

K = 0.40

SOUND = NO DATA

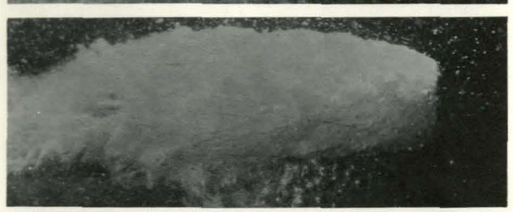

(i)

K = 0.53

SOUND = NO DATA

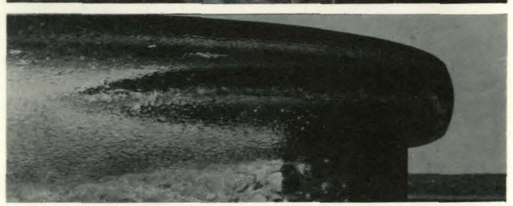

(j)

K = 0.46

SOUND = NO DATA

(k)

K = 0.47

SOUND = NO DATA

(l)

K = 0.44

SOUND = NO DATA

29 28 27 26 25 24 23 22 21 20 19 18

DISTANCE ALONG AXIS, INCHES

FIG. 22

CONFIDENTIAL

CAVITATION
ON SEMI-ELLIPSOID NOSE

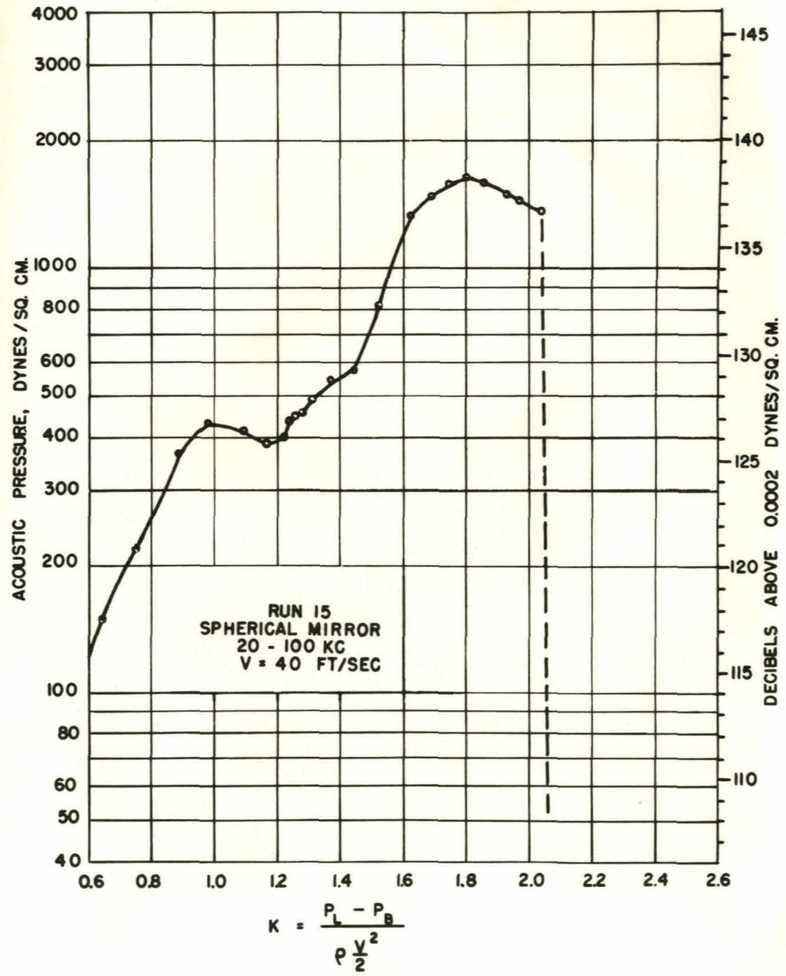

CONFIDENTIAL

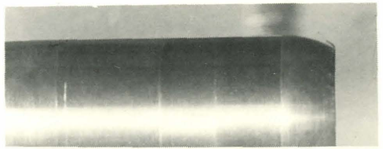

ENLARGEMENT OF FIG. 23a
WITH SMALL WISPS OF CAVITATION
ACCENTUATED

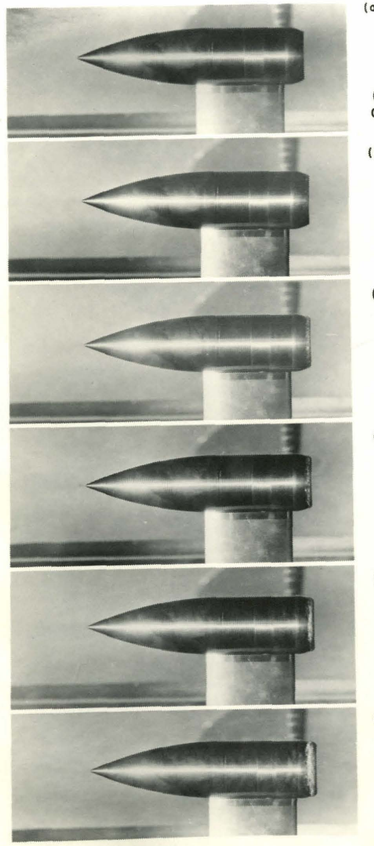

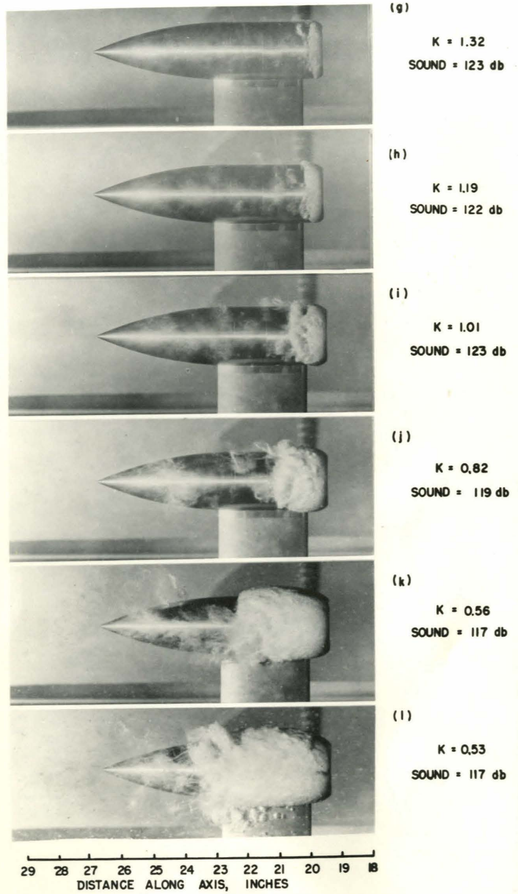

FIG. 23

CONFIDENTIAL

CAVITATION
ON TRUNCATED HEMISPHERE NOSE

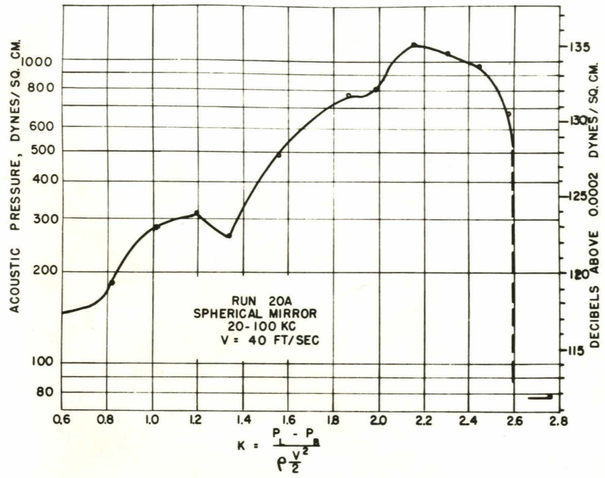

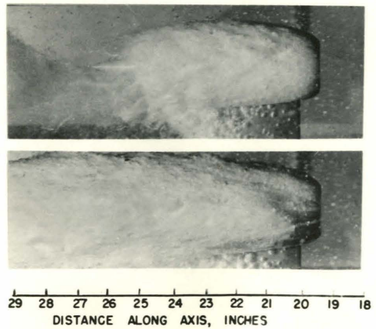

CONFIDENTIAL

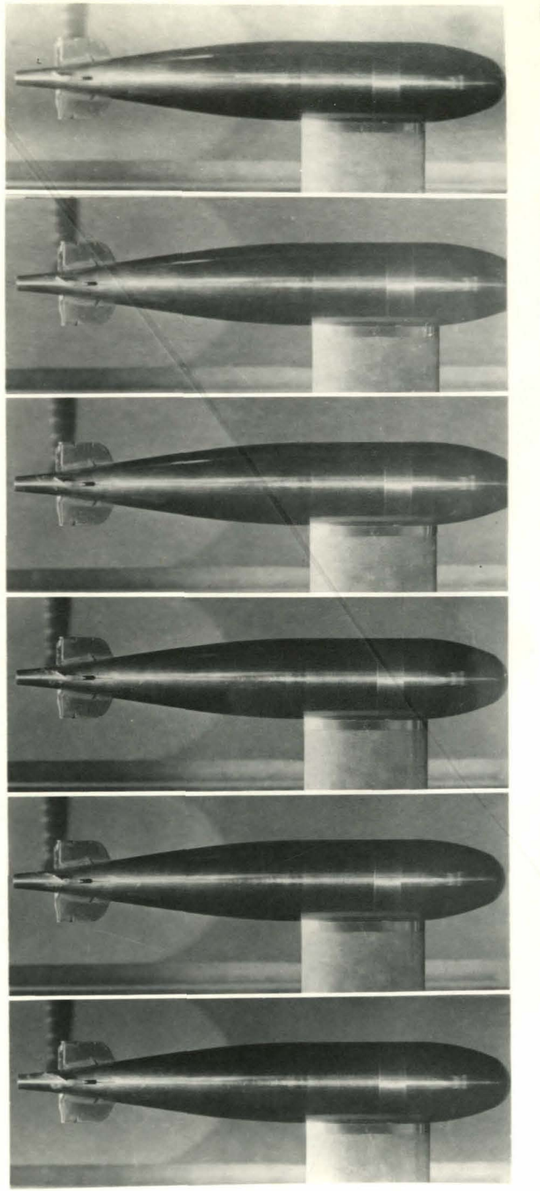

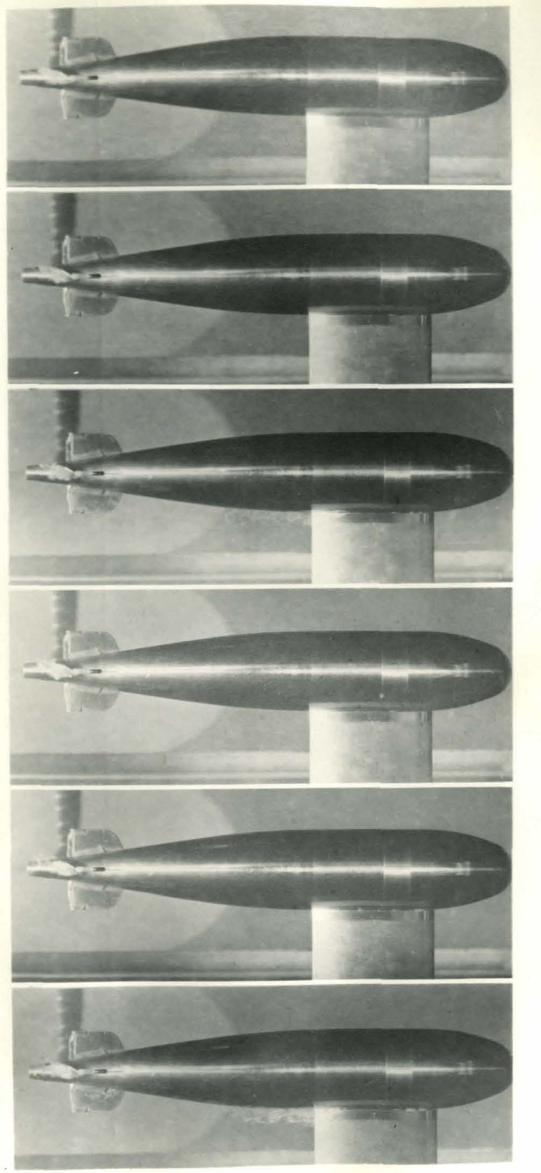

FIG. 24

CONFIDENTIAL

CAVITATION

ON UP TURNED RUDDER OF FIN TAIL

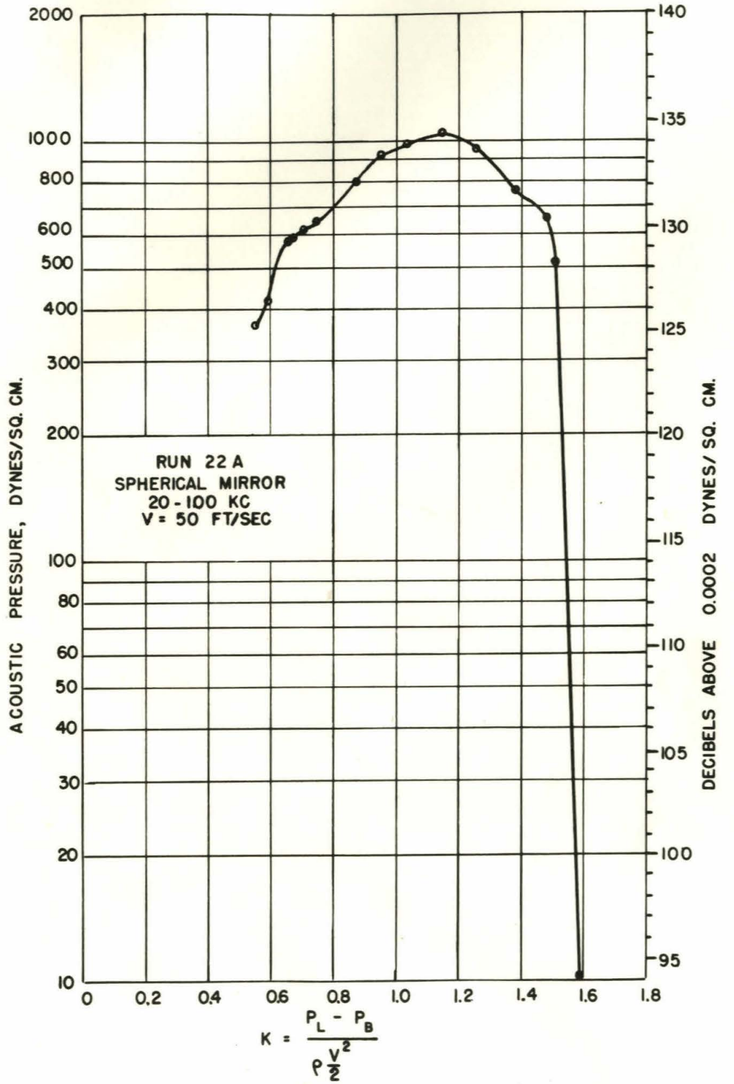

CONFIDENTIAL

COMPARISON OF FOUR TYPES AT SAME VELOCITY

It should be noted again that each set of data in Figures 21 to 24 is for a different velocity and, furthermore, the inception of cavitation occurs at a different pressure for each body. Consequently, there is no satisfactory basis for comparison of the magnitudes of the sound levels measured. Measurements of the noise produced by each of the projectiles at the same velocity of 47 ft/sec were obtained using the ellipsoidal reflector instead of the spherical mirror. These results are shown in Figure 25. The

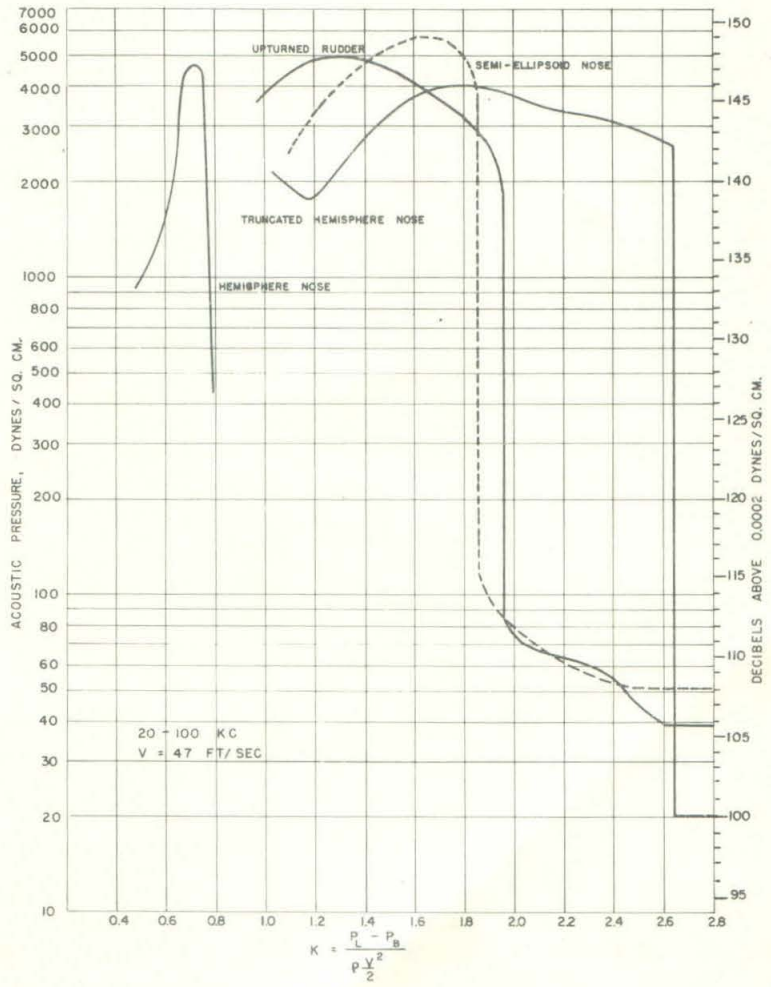

FIG. 25 NOISE CAUSED BY CAVITATION ON FOUR PROJECTILES

increased effectiveness of this reflector over the spherical mirror is apparent. For example, the hemisphere nose curve shows a maximum sound pressure of 4800 dynes per square centimeter for this 47 ft/sec test, as against about 1100 shown in Figure 21 for a 60 ft/sec test with the spherical mirror. Similarly higher peaks are obtained for the others. These curves show some difference in the magnitudes of the noise peaks for the different bodies. There is also some differencc in the shapes of the curves, the peak occurring at a K somewhat lower than the inception value for the two most abrupt shapes, the truncated hemisphere and the upturned rudder. For the hemisphere and the semiellipsoid the peak occurs soon after the inception point. The sharp discontinuities also show the most sensitivity to change in K near the inception point. For both the truncated hemisphere and the upturned rudder, the determination of the beginning of cavitation was very critical so that sound measurements in that region were difficult to obtain. With the other two noses, however, the increase, while sudden, could be traced and with extreme care measurements made at levels intermediate between the background and highest pressures.

NOISE VS. VELOCITY

In Figure 26 are curves for the hemisphere nose showing the change in noise with velocity. For the velocity range of 40 to 70 ft/sec the increase in maximum noise for each speed is approximately linear. This holds for both the 20 to 100 kc and 80 to 100 kc frequency bands. This maximum noise is not obtained at the same pressure (submergence) for all speeds, but rather at nearly a fixed value of the cavitation parameter, K. If a projectile travels under water at a fixed depth, the maximum noise represented by the straight lines in Figure 26 will be generated only at one velocity where K assumes the above fixed value. For all other velocities the noise will be less than the maximum. The other curves in Figure 26 show the variation in noise in 20 to 100 kc band for this nose submerged to 10 feet and 15 feet. It will be noted that the noise level is low up to the criticdl velocity for inception of cavitation where it increases several fold to the maximum level curve shown. Beyond this peak a reduction occurs. Of course, cavitation is postponed to higher

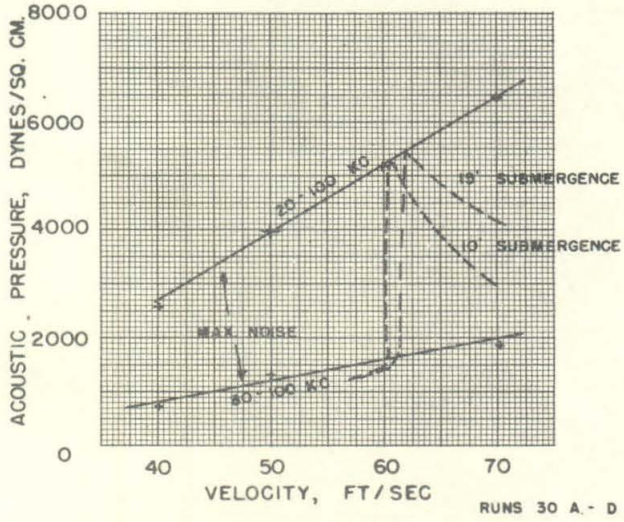

FIG. 26 NOISE VS. VELOCITY
Hemisphere Nose

velocities as submergence increases, but when cavitation does occur, the peak noise is higher also. It might be noted that the data from which these curves were drawn were obtained with a different arrangement in the Water Tunnel setup, so the magnitudes of the maximum noise are not directly comparable to those illustrated in Figure 25.

NOTE ON MAGNITUDE OF MEASURED NOISE

It should be emphasized that the absolute magnitudes of the sound levels measured in the Water Tunnel bear no particular relation to what might be obtained in the field. In any event, in either laboratory or field measurements the hydrophone receives only such a portion of the total sound emitted as the geometry of the setup permits. The magnitudes reported here are good for comparative purposes only.

B. LOCATION OF NOISE SOURCE DURING CAVITATION

VISIBLE CAVITATION AND THE NOISE SOURCE

It is generally agreed that on the collapse of cavitation bubbles a large store of energy is released, and that at the point of energy concentration very high local pressure intensities are obtained. The resulting high frequency pressure waves are the cause of the mechanical damage commonly known as "cavitation corrosion" and of noise, both acoustic and supersonic.(7) That the source of noise measured is concentrated at the zone where cavitation is visible is clearly shown by traverses giving the sound pressure as the hydrophone is moved parallel to the Water Tunnel axis. As the examples for the hemisphere nose in Figure 27 show, when the hydrophone is positioned to focus on the cavitation zone in the photographs, the maximum noise level is obtained. At 1" on either side of this position the sound is reduced 3 to 5 db. The ring source shown in the photographs appears as a line to the hydrophone receiver so that, as might be expected, focusing of the hydrophone in a position 1" above or below the center line of the working section gives less than a 1 db reduction in the level. The measurements in Figure 27 are for the 80 to 100 kc band because, as the curves already presented in Figure 14 show, the most pronounced focusing was obtained at the higher frequencies. Figure 14 also shows that the maximum sound pressure is obtained at the same position regardless of frequency.

MOVEMENT OF SOURCE WITH SHIFTING ZONE OF COLLAPSE

If it is assumed that the bulk of the total noise measured from a cavitating object is obtained from the collapse of the bubbles, the physical observation that the collapsing zone moves downstream with the growth of cavitation should indicate the movement of the noise zones. The curves in Figure 27 also indicate this trend. The peak obtained for a cavitation parameter, K, of

O.56 is approximately 1/2" farther back than the peak for K = O.73, whereas photographs of Figures 21 (c) and 21 (g) indicate about O.6" downstream elongation of the cavitating zone.

It has been suggested that growth of the sound source could indicate an apparent shift in its location, or that some combination of the effects of the screening and reflections peculiar to the projectile and tunnel configuration could explain the measured shift. It is felt, however, the agreement between length of cavitation bubble and movement of the sound peak measured in this and other cases is good evidence that the noise source is moving with the collapsing trail of bubbles.

Measurements for the cut hemisphere nose in Figure 28 show the same typical trends observed with the hemisphere nose. In Figure 29 are shown the results obtained with cavitation on the upturned rudder. These curves do not indicate a consistent shift in peak, even though cavitation at the lowest K is much more severe than at the highest. Reference to Photographs 24 (h), 24 (i), and 24 (j) show, however, that the visible zone of vapor

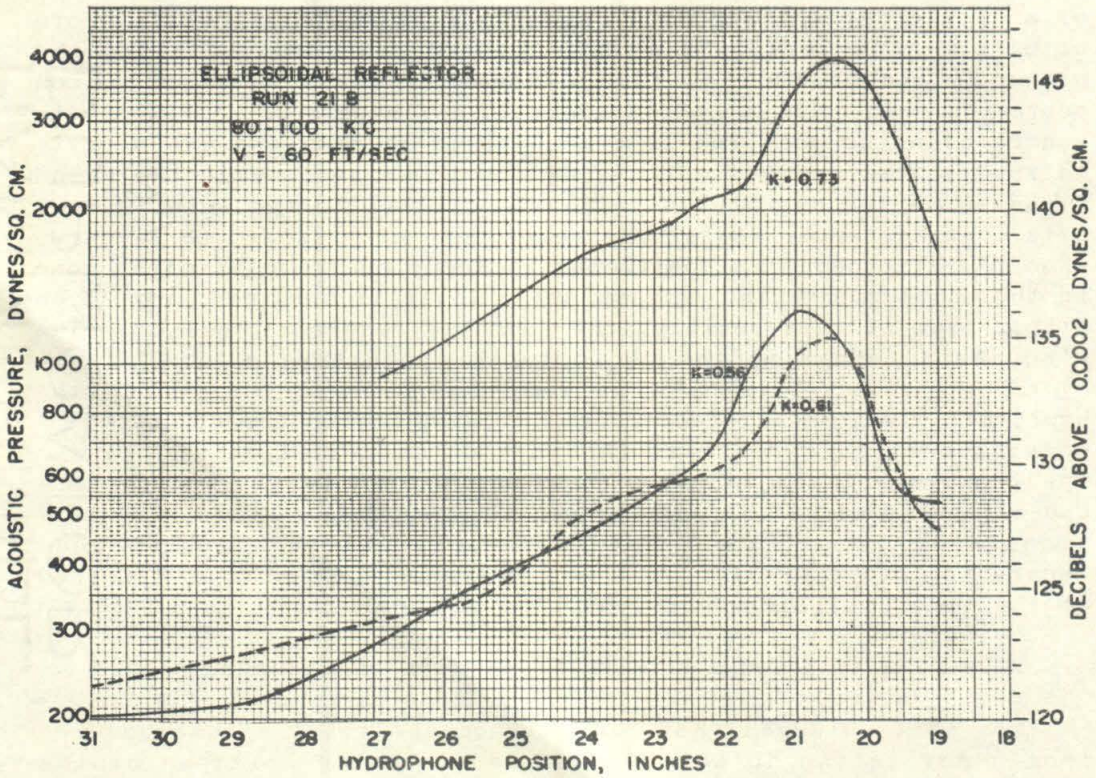

FIG. 27 MOVEMENT OF NOISE SOURCE WITH GROWTH OF CAVITATION ON THE HEMISPHERE NOSE
Compare with Fig. 21 (c), (f), (g)

on the lee of the rudder was changed very little as K was reduced. With more severe conditions, more and more vapor was entrainedby the water and swept downstream to collapse outside the range of the hydrophone system, but the main cavity shown was almost uninfluenced.

In Figures 27 to 29 only the relative position of the noise peaks is indicated. Definite determination of the exact position of the zones was not possible since, in mounting the hydrophone reflector assembly, the possible errors in angular adjustment in the horizontal plane could contribute as much as the indicated difference between the hydrophone position and the cavitation zone when the peak noise was measured. Measurements made with a given installation, however, gave good comparative results since the whole assembly was attached to a carriage which could be moved parallel to the tunnel on machined rails.

The effect of the movement of the sound peak with the growth of cavitation has a secondary effect on the accuracy of the sound vs. K curves shown in Figures 21 to 25, which were obtained with

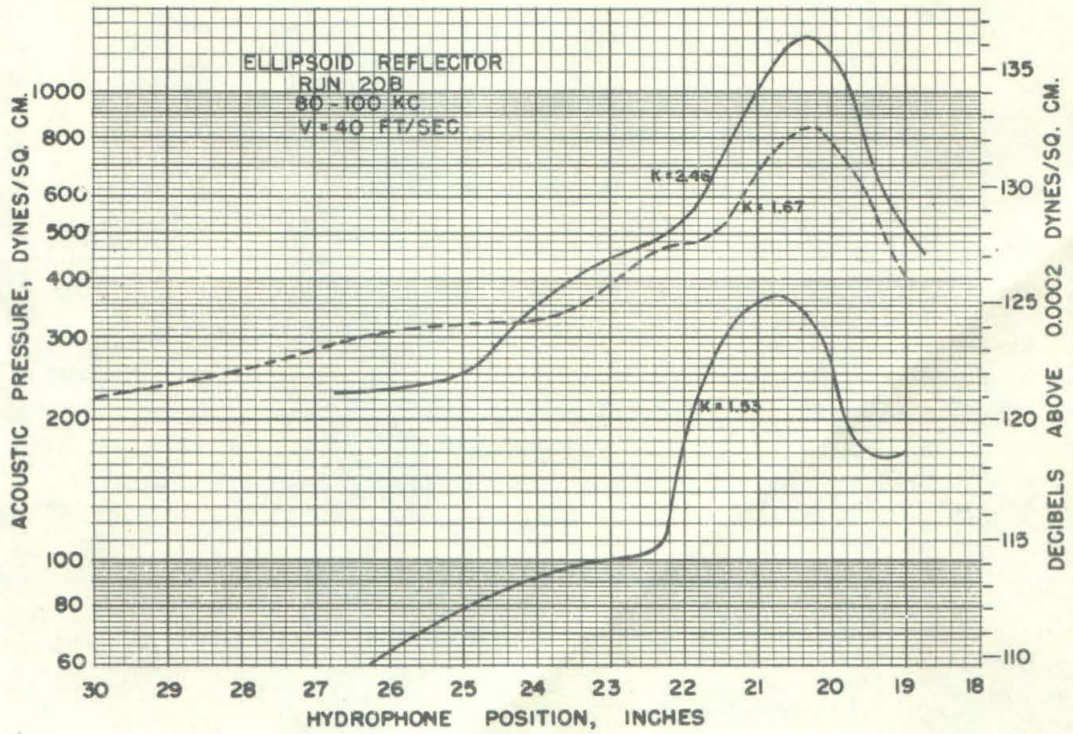

FIG. 28 MOVEMENT OF NOISE SOURCE WITH GROWTH OF CAVITATION ON THE TRUNCATED HEMISPHERE NOSE
Compare with Fig. 23 (a), (f)

the hydrophone in a fixed position. With the growth of the cavitation zone beyond the amount giving the maximum noise, the level measured by the fixed hydrophone is slightly low. This effect is small, however, being less than 2 db for the hemisphere nose at K = 0.56 or the truncated hemisphere at K = 1.51. Consequently, it does not alter the peculiar characteristics of the measurements shown nor change the conclusions already presented.

It is interesting to note that in Figures 27 to 29 the sound pressure location curves for the hemisphere nose and tail rudder showed more gradual reductions in noise on the side of the maximum which was toward the body of the model. This asymmetry became more pronounced at lower K values, while at high K's, as obtained with the cut hemisphere nose in Figure 28, no definite asymmetry is observed. Examination of the photographs in each figure shows that at the lowest K's, cavitation is occurring at the junction between the streamlined strut which supports the projectile and the cylindrical projectile body. It is thought that this secondary cavitation is contributing to the measured sound and is responsible for the asymmetry observed.

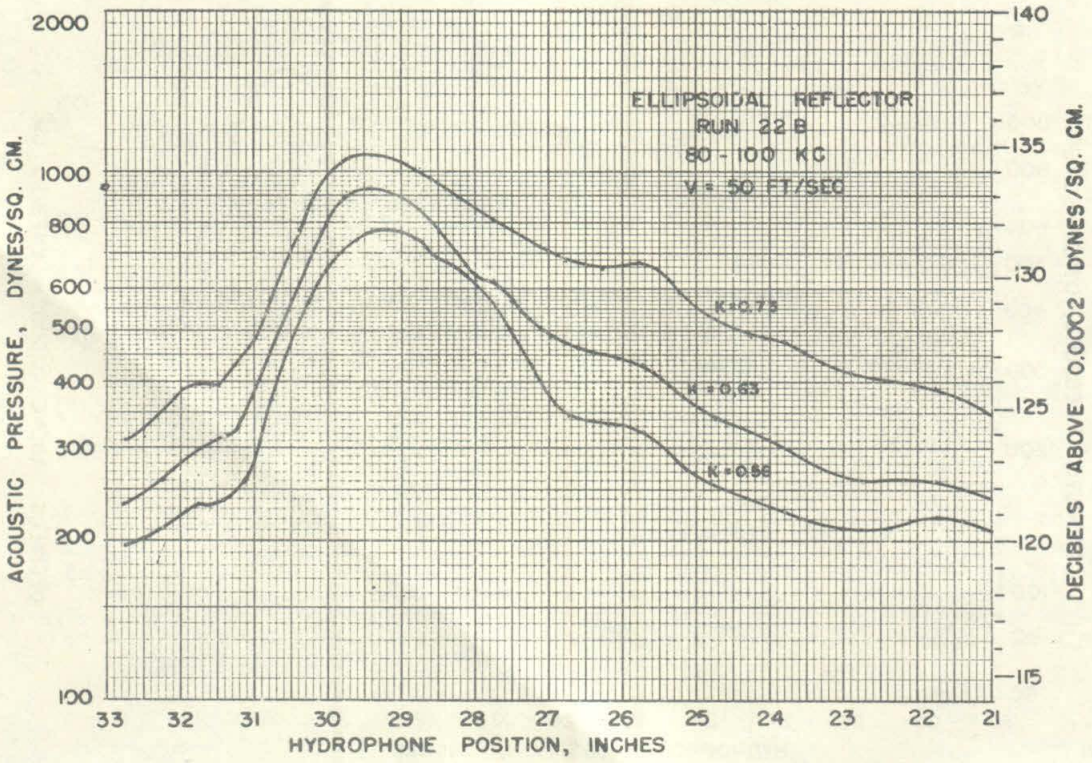

FIG. 29 MOVEMENT OF NOISE SOURCE WITH GROWTH OF CAVITATION ON UPTURNED RUDDER OF FIN TAIL
Compare with Figures 24 (h), (i), (j)

APPENDIX I

DESCRIPTION OF TEST PROCEDURE AND METHOD OF PRESENTING DATA

For the investigation of the noise from cavitating projectiles, two types of sound measurements were made. One objective was to measure the sound pressure of the noise as cavitation developed. for this test, the model was mounted in the tunnel and a constant velocity flow was established. A small amount of cavitation was produced by lowering the pressure in the working section and the hydrophone reflector assembly was positioned to give a maximum reading. Then the pressure in the tunnel was raised until cavitation disappeared completely. The water pressure was then reduced again by small steps, and cavitation developed. At each setting, the absolute water pressure and the sound pressure were measured. The water pressure was always reduced when data were taken in order to avoid a hysteresis effect in the formation and disappearance of cavitation which occurs for some conditions (4) Flash photographs of about a 20 microsecond exposure were taken at each stage of the cavitation. Tests of this type were performed with various velocities, and sound pressure was measured in different frequency bands.

The second objective was to measure the variation in sound pressure along a line parallel to the axis of the tunnel for various degrees of cavitation on the nose, body or tail of the model. During these experiments, water pressure and velocity were held constant, and the sound pressure was recorded as the hydrophone and sound reflector were moved parallel to the axis of the tunnel. The focused direction was held normal to this axis and, hence, normal to the lucite window of the working section. Tests of this type were performed for various values of water pressure, velocity, and also with different frequency channels.

In addition, in order to measure the background noise, tests of both types were performed without a model or a strut in the working section.

The amplifiers were calibrated before and after each test by introducing a known voltage in series with the hydrophone and measuring the output.

The influence of pressure and velocity on the inception and development of cavitation is represented conveniently by a parameter defined as

$$K = \frac{P_L - P_B}{\rho \frac{V^2}{2}}$$

where

P_L = absolute pressure in the undisturbed flow in lbs/sq ft

P_B = absolute pressure in the cavitation bubble, taken in these tests as the vapor pressure of the liquid, in lbs/sq ft

ρ = density of the fluid in slugs/cu ft

V = velocity in ft/sec

The quantity, $P_L - P_B$, is the margin of pressure above that at which local boiling and, hence, cavitation can occur. The dynamic pressure, $\rho \frac{V^2}{2}$, is a measure of the possible local pressure reduction caused by local flow accelerations on the model. Thus, either a decrease in P_L, or an increase in V, will produce a tendency to cavitate. Each advanced stage of cavitation is described by successively lower values of K, and the degree and general appearance of the cavitation can be reproduced by adjusting pressure and velocity to give the desired K. For the constant speed tests reported here, a variation in pressure causes a proportional change in K.

Sound pressure is the term used to describe the acoustic pressure in dynes per square centimeter of the noise produced by cavitation. Values of sound pressure measured by the hydrophone are stated in decibels above the standard reference level of 0.0002 dynes per square centimeter.

By plotting the measured acoustic pressure against the cavitation parameter, K, a semidimensionless representation of results is obtained. At any K along the abscissa, a cavitation zone having a characteristic overall geometry is described regardless of velocity and pressure. The magnitude of the sound pressure shown, however, holds only for the given velocity of test.

APPENDIX II

REFERENCES

(1) "Measurements of the High Frequency Noise Produced by Cavitating Projectiles in the High Speed Water Tunnel" by R. T. Knapp, HML Report ND-8.2, Section No. 6.1-sr207-924, August 31, 1943

(2) "The High Speed Water Tunnel at the California Institute of Technology" by R. T. Knapp, V. A. Vanoni, and J. W. Daily, HML Report ND-1, June 29, 1942

(3) "Mechanical and Acoustic Attachments for Piezoelectric Crystals used in Transducers", Section No. 6.1-sr346-628, December 15, 1942. See Section V on "Use of Plastics as Sound Transmitting Media"

(4) "Dictionary of Underwater Acoustical Devices". A report prepared by Columbia University Division of War Research, Underwater Sound Reference Laboratories, Section No. 6.1-sr20-889, July 27, 1943

(5) "Measurements on a C11-A1 Hydrophone with an Ellipsoidal and a Spherical Reflector". A report prepared by the Calibration Group of the University of California Division of War Research, October 30, 1944, UCDWR No. C64

(6) "Flow Diagrams of Projectile Components" by G. Van Pelt and E. Thorne, HML Report No. ND-36, Section No. 6.1-sr207-1649, September 15, 1944

(7) "Experimental and Theoretical Investigation of Cavitation in Water" by J. Ackeret, Report of the Kaiser Wilhelm Institute für Strömungsforschung, Göttingen, January 1930, Techn., Mechan, und Thermodynamik, pp. 1-22, Vol. 1